UNIVERSITÀ
DEGLI STUDI
DI PADOVA

Sede Amministrativa:

Università degli Studi di Padova

Dipartimento di Medicina Molecolare

Corso di dottorato di ricerca in Medicina Molecolare

Curricolo Biomedicina

Ciclo XXXI

Role of YAP/TAZ downstream of common oncogenic drivers

Tesi redatta con il contributo finanziario di Fondazione Cariparo

Coordinatore: Ch.mo Prof. Stefano Piccolo

Supervisore: Ch.mo Prof. Stefano Piccolo

Dottorando : Dott.ssa Anna Citron

Index

Index 3

Publications 5

Abstract (English) 7

Abstract (Italiano) 9

Introduction 11

YAP/TAZ biological roles *11*

YAP/TAZ in cancer *11*

Pancreatic cancer 12

Breast cancer 13

YAP/TAZ regulations *14*

YAP/TAZ regulation by Hippo pathway and cell polarity 14

YAP/TAZ and Wnt pathway crosstalk 15

YAP/TAZ and glucose metabolism 16

YAP/TAZ in mechanotransduction 16

Hypotheses and aim 19

Results 21

I) YAP/TAZ transcriptional activity is promoted by KRas and HER2 overexpression. *21*

II) YAP/TAZ are mediators of the initial steps of tumorigenesis *22*

II.II) YAP/TAZ are required for KRas mediated cell transformation of pancreatic acinar cells 22

II.III) YAP/TAZ mediates cell plasticity conferred by HER2 overexpression in mammary gland luminal cells 24

III) Targeting mechanotransduction as a strategy to inhibit oncogene mediated YAP/TAZ activation *26*

III.I) KRas tumorigenic effect relies on YAP/TAZ mechanotransduction 26

III.II) YAP/TAZ as therapeutic target to inhibit KRas mediated tumorigenesis 28

IV) Soft extracellular matrix inhibits tumor growth in vivo *29*

IV.I) Lysyl Oxydase inhibitor blunts tumor overgrowth in a mammary carcinoma mouse model 29

IV.II) Lysyl Oxidase inhibitor treatment reduces progression of Pancreatic Adenocarcinoma in vivo 30

V) Members of the Angiomotin protein family are YAP/TAZ mechano-regulators 31

V.I) Angiomotins behave as YAP/TAZ inhibitors in classical mechano-assays 32

V.II) Angiomotins inhibit YAP/TAZ in response to cytoskeletal modifications 33

Conclusions 35

Experimental procedures 39

References 47

Figures 53

Acknowledgments 81

Publications

Brusatin, G., Panciera, T., Gandin, A., Citron, A., and Piccolo, S. (2018). Biomaterials and engineered microenvironments to control YAP/TAZ-dependent cell behaviour. Nat. Mater. 17, 1063–1075

Abstract (English)

YAP and TAZ are transcriptional coactivators that play a central role in cancer initiation and growth. Despite being widespread activated in a number of human malignancies, YAP/TAZ aberrant triggering is rarely due to genetic alteration, but it is likely occurring as a consequence of mis-regulation of the complex network of signaling pathways that converge on these factors. We thus asked if recurrent oncogenic lesions, that are considered as tumorigenic drivers, might work though YAP/TAZ to induce cell transformation. We found that YAP/TAZ are not only activated upon oncogenic stimulation, but are required for the onset of malignant phenotypes induced by oncogenes in carcinogenesis models both *in vitro* and *in vivo.* Interestingly, we also found that the physical composition of the extracellular environment is crucial to allow oncogenes to foster tumor initiation and progression, by sustaining YAP/TAZ activity. Indeed, cells that are not able to properly organize F-actin cytoskeleton are refractory to oncogene-induced transformation. The finding that YAP/TAZ are the molecular nexus on which different tumorigenic drivers converge, and that oncogenes mediated transformation requires proficient transduction of mechanical signals to YAP/TAZ, might have relevant implications for the identification of a common molecular target to inhibit tumor onset.

Abstract (Italiano)

YAP e TAZ sono due co-fattori trascrizionali che rivestono un ruolo centrale nell'insorgenza e nella crescita del tumore. Nonostante siano ampiamente iper-attivati in diversi tipi di neoplasie, l'attivazione patologica di YAP/TAZ è raramente attribuibile a mutazioni genetiche, ma è più probabilmente dovuta ad alterazioni nel complesso network di cascate del segnale che partecipano alla regolazione di questi fattori. Ci siamo quindi chiesti se alterazioni genetiche che sono frequentemente riscontrate in cellule tumorali, e che sono per questo considerate iniziatori dei processi di tumorigenesi, possano sfruttare l'attivazione di YAP/TAZ. Abbiamo scoperto che YAP/TAZ non solo sono attivati a valle di diversi oncogeni, ma che sono necessari per l'insorgenza di fenotipi aberranti dovuta all'attivazione di oncogeni in modelli di carcinogenesi sia *in vitro* che *in vivo.* Abbiamo inoltre scoperto che la composizione fisica dell'ambiente extra-cellulare è rilevante per permettere agli oncogeni di promuovere l'insorgenza e la crescita tumorale, perché partecipa a sostenere l'attivazione di YAP/TAZ. Cellule che non sono in grado di ri-strutturare efficientemente il citoscheletro sono infatti più refrattarie al processo di trasformazione. L'identificazione di YAP/TAZ come fattori centrali su cui converge l'attività di diversi oncogeni, e la scoperta che la trasformazione cellulare indotta da questi richiede un'efficace trasduzione di segnali meccanici per attivare YAP/TAZ, possono avere importanti implicazioni per lo studio di nuovi target molecolari comuni, che possano essere sfruttati per inibire la crescita di diversi tipi di neoplasie.

Introduction

YAP/TAZ biological roles

YAP/TAZ are two related transcriptional coactivators, that shuttle between the cytoplasm and the nucleus, where they interact with other transcription factors, as the TEA domain members (TEAD), to promote transcription of their target genes. YAP/TAZ/TEAD control target genes expression mainly by recruitment to distant enhancers, regulating their target promoters through DNA looping (Zanconato et al., 2015). YAP/TAZ have been classically described as regulators of organ size; embryonic hyperactivation of YAP/TAZ in genetically engineered mouse models results in tissue overgrowth spurred by enhanced cell proliferation (Harvey et al., 2003). But YAP/TAZ are also involved in processes such as tissue regeneration and repair upon injury, or maintenance of tissue specific stem cell pools. For example, recently YAP/TAZ have been recognized as key mediators of tissue regeneration in the intestinal epithelium, in which they induce the reprogramming of adult epithelial cells into fetal-like progenitors (Yui et al., 2018). More in general, YAP/TAZ overexpression in adult differentiated cells is sufficient to reprogram them into the tissue specific somatic stem cells (Panciera et al., 2016). A novel function of YAP/TAZ is thus suggested by this evidence, that is the ability to induce cell plasticity in adult cells to endow stemness properties. Increasing interest is also raising from their emerging role as promoters of tumorigenic features. Indeed, YAP/TAZ are widespread activated in several human solid malignancies, where they are essential in conferring cancer stem cells traits, and are mediators of aberrant proliferation, chemoresistance and promoters of metastatic invasion (Fig. 1A) (reviewed in Zanconato et al., 2016).

YAP/TAZ in cancer

As mentioned above, YAP/TAZ are key mediators of several of the features of cancer cells; one of the most relevant is aberrant cell proliferation. In particular, this response in cancer cells is mediated by a specific transcriptional program in which a significant part of YAP/TAZ direct target genes are encoding for proteins related to cell-cycle progression (Camargo et al., 2007; Zhao et al., 2008). This program allows transcription of proteins involved in replication, DNA synthesis and repair, control of S-phase checkpoint, and mitosis accomplishment. YAP/TAZ hyperactivation can also avoid anoikis induced by cell detachment (Zhao et al.,

2012), another classical hallmark of cancer cells. Moreover, YAP/TAZ can block either mitochondrial-dependent or alternative apoptosis cascades by upregulating Bcl2-family members (Rosenbluh et al., 2012). On the other hand, YAP/TAZ can avoid senescence of cancer cells by constantly promoting minimal levels of autophagy (Song et al., 2015), but still inhibiting cell death caused by over-activation of autophagy in the tumor bulk (Liang et al., 2014). YAP/ TAZ are also related to the tumor's pool of cancer stem cell (CSC), of which they are the molecular determinants. Indeed, they are responsible for the acquisition of CSC features in non-stem tumor cells and are then required for CSC expansion (Cordenonsi et al., 2011). However, YAP/TAZ are fundamental not only for the population of tumor cells, but can induce malignant phenotypes also in cells of the tumor stroma, fostering a continuous development of the disease. Indeed, YAP/TAZ are overexpressed in cancer-associated fibroblasts (CAFs), where they stimulate the production of inflammatory interleukins and promote the deposition of ECM proteins. This installs a feedforward loop to self-sustain YAP/TAZ activity in both tumoral and stromal cells (Calvo et al., 2013; Halder et al., 2012), promoted by mechanical activation of YAP/TAZ by the rigid ECM (as will be discussed below) (Fig. 2A). In summary, YAP/TAZ are recognized as key tumor promoting factors as well as determinants of the chemical, physical, and cellular composition of the overall tumor environment. Indeed, YAP/TAZ are hyperactivated in the majority of solid malignancies, as for example in breast cancers (BC), colorectal cancers, gastric cancers, pancreatic cancers, gliomas, prostate cancers, endometrial carcinomas, melanomas, mesotheliomas, osteosarcomas and in several kinds of brain tumors (Fig. 1A) (Zanconato et al., 2016). In this work, we focused on two specific tumors, that are pancreatic ductal adenocarcinoma and breast cancer.

Pancreatic cancer

Pancreatic-ductal adenocarcinoma (PDAC) is one of the most common causes of cancer-related death, with 6% 5-year survival rate and increasing incidence associated with metabolic disorders. The high lethality of PDAC resides in the lack of timely diagnosis and ineffective treatment for more advanced tumors. PDAC is the last stage of a progressive course of carcinogenesis, that develops from precursor lesions, the most common of which are microscopic pancreatic intraepithelial neoplasias (PanINs). PanINs can be classified in two categories; low-grade (PanIN-1 and PanIN-2) and high-grade (PanIN-3), which identify the

increasing potential for progression of the two subgroups (Ying et al., 2016). YAP and TAZ are expressed and nuclearly localized in PanINs and in some subtypes of PDAC, and strongly accumulated in the nuclei of cells from PDACs derived metastases. This is true for human lesions, for PanIN and PDACs arising in mouse models of pancreatic cancer, and for human PDAC derived cell lines growing as xenografts (Diep et al., 2012; Morvaridi et al., 2015). It is also reported that pancreas-specific *Yap* knockout can inhibit tumor growth from low-grade PanIN to PDAC in mouse models (Zhang et al., 2014). A peculiar feature of PDAC is the presence of a massive desmoplastic stroma, accounting for more than 90% of the total tumor volume. Pancreatic stellate cells (PSCs) are the most represented fibroblasts in the PDAC stroma. In the healthy pancreas, PSCs, by secreting metalloproteinases (MMPs), have an important role in the turnover and in the architecture of the ECM. Upon pancreatic injury, such as chronic pancreatitis or during the development of a PDAC, PSCs increase ECM production and acquire a myofibroblast-like phenotype. Activated PSCs are responsible for an excessive deposition of ECM components, leading to the classical fibrotic landscape observed in PDAC (Ying et al., 2016).

Breast cancer

Breast cancer (BC) is the most common cancer diagnosed in women, with an incredible high incidence: one woman out of nine is expected to develop breast cancer in her lifetime (Marcotte and Muller, 2008). Genetic analyses of tumoral cells in sporadic breast cancer showed that these bear several different genetic lesions, including loss of heterozygosity of DNA regions that contains putative tumor suppressor genes, and regions of DNA amplification, likely containing oncogenes. These breast cancers are mostly carcinomas that originate from epithelial cells lining the ducts of mammary glands. BC progresses through different stages, starting from atypical hyperplasia, becoming ductal carcinoma *in situ* and finally invasive ductal carcinoma. Late stage BC are also related to metastases to distant organs, that are usually the cause of breast-cancer related death. Invasive ductal carcinomas are classified into different subgroups: hormone (estrogen and/or progesterone)-receptor-positive BC, HER2-positive BC, and BCs that are negative for all three receptors (triple-negative BC, or TNBC). In BC, YAP/TAZ signatures are correlated with high histological grade, increased rate of metastases onset, and poor outcome (Marcotte and Muller, 2008). TAZ is accumulated in the nuclei of cells in high-grade BC and is prognostic of poor clinical

outcome, in particular in TNBC (Bartucci et al., 2015; Cordenonsi et al., 2011). In transgenic mouse models of mammary tumor, nuclear YAP/TAZ are induced in tumors caused by expression of HER2, Wnt1, or Polyoma-middleT (PyMT, a tumorigenic driver that originates carcinomas similar to HER2 tumors from a molecular standpoint). In the MMTV-PyMT mouse model, conditional knockout of YAP in the mammary gland increases the latency and reduces the growth of mammary carcinomas (Chen et al., 2014; Serrano et al., 2013). As mentioned above, TAZ overexpression in benign BC cell lines increases the number of tumor-initiating cells, allowing them to form high-grade tumors after injection in the mammary fat pads of immunocompromised mice. Moreover, TAZ overexpression confers metastatic abilities to primary human BC cells that are normally low tumorigenic (Bartucci et al., 2015; Cordenonsi et al., 2011). These studies suggest that YAP/TAZ may play an important role in BC development, promoting the acquisition of CSC features, and sustaining malignancy and metastatic relapse.

YAP/TAZ regulations

Despite their widespread activation in tumors, mutations in the coding sequences of *YAP* or *TAZ* have not been reported in human cancers, with the sole exception of gene amplifications very rarely observed in specific tumors, such as in the case of some types of breast cancer, hepatocellular carcinoma, mesothelioma and nonsmall cell lung cancer (Zanconato et al., 2016). An instructive insight into their pathological role may thus be achieved by considering their diverse regulatory pathways.

YAP/TAZ regulation by Hippo pathway and cell polarity

The Hippo pathway is the first discovered regulatory pathway for YAP/TAZ. The core cassette of the mammalian Hippo pathway is composed of two kinases: MST1/2 and LATS1/2. MST1 and MST2 (orthologues of Hippo in *Drosophila)*, in cooperation with their binding partner SAV1, directly phosphorylate large tumor suppressor 1 (LATS1) and LATS2 (orthologues of Warts in *Drosophila*) stimulating their activation. LATS proteins, aided by the co-factor MOB-1, in turn phosphorylate YAP/TAZ causing their cytoplasmic retention and protein degradation (Harvey et al., 2003). Interestingly, some of the upstream inducers of the Hippo pathway are involved in cell-cell adhesion and polarity. In epithelial cells Merlin is located at cell–cell junctions to strengthen adhesion and is a potent inducer of the Hippo

pathway, serving as scaffold for the core kinase cassette (Yin et al., 2013). Similarly, Scribble, another cell polarity key factor, acts as adaptor to recruit and activate MST and LATS. Indeed, epithelial architecture, with the engagement of cell-cell junctions and polarity, is considered as an inhibitor of YAP/TAZ. On the other hand, loss of cell polarity is a common feature of epithelial–mesenchymal transition (EMT), an alteration in cell morphology that is associated to change of fate and acquisition of stemness traits and related to Scribble delocalization. In line, YAP/TAZ are activated upon EMT and are required to confer cancer stem cell attributes downstream of epithelial–mesenchymal transition (Cordenonsi et al., 2011). Several observations, however, suggest that, even if the Hippo pathway is a regulator of YAP/TAZ activity, it might not be the main player of YAP/TAZ-modulation in diverse physiological and pathological conditions. Indeed, several LATS-independent layers of regulation are reported, such as RhoGTPase signalling, inflammation, metabolism and mechanotransduction (reviewed in Panciera et al., 2017; Totaro et al., 2018). This suggests that a single pathway is not sufficient to activate YAP/TAZ, but a combination of inputs, Hippo-dependent and -independent, must accumulate to promote YAP/TAZ activity. For example, YAP phosphorylation of the LATS-target S127 residue does not prevent YAP nuclear localization (Wada et al., 2011), and phosphorylated YAP, that should be cytoplasmic retained, can be found accumulated in the nucleus upon inhibition of nuclear export (Ren et al., 2010). Hippo pathway can thus be considered as one branch of a broad network of regulatory events.

YAP/TAZ and Wnt pathway crosstalk

Besides their role as effectors of the Hippo pathway, YAP/TAZ are also activated downstream of other signals, such as the canonical Wnt pathway, in particular to promote their shared transcriptional programs related to cell proliferation and tumorigenesis. The cytoplasmic "destruction complex" is the core of the Wnt pathway, and controls intracellular levels of β-catenin: when Wnt ligand is present, it inactivates the destruction complex allowing β-catenin transcriptional activity. YAP/TAZ have also been described as members of the destruction complex, in which they promote the recruitment of β-transducin repeats-containing protein (β-TRCP), inducing β-catenin degradation (Azzolin et al., 2014). On the other hand, in conditions in which YAP/TAZ nuclear translocation is favored, also β-catenin nuclear accumulation is promoted. This suggests the presence of a crosstalk between Wnt pathway

and other YAP/TAZ activating signals, possibly aimed to ensure that specific responses, such as aberrant proliferation and acquisition of tumorigenic features, are induced only in presence of coherent inputs. This case is exemplified by intestinal adenomas emerging upon APC mutation, one of the components of the destruction complex. APC loss prevents the assembly of the destruction complex, promoting YAP/TAZ nuclear accumulation, that is essential for the development of the tumor. Indeed, YAP/TAZ are required in a mouse model of colorectal cancer downstream of APC depletion (Azzolin et al., 2012). On the other hand, hyper-accumulation of TAZ and β-catenin in mouse intestinal cells results in the formation of adenomas, similar to those induced by *Apc* mutations (Cai et al., 2015).

YAP/TAZ and glucose metabolism

Glucose availability has been recently found to promote YAP/TAZ activity, since high levels of glucose lead to production of uridine diphosphate *N*-acetylglucosamine (UDP–GlcNAc), that is employed in YAP *O*-GlcNAcylation, which, in turns, stabilize YAP protein levels (Enzo et al., 2015). Moreover, phosphofructokinase 1 (PFK1), one of the kinases of the glycolytic cascade, promotes YAP/TAZ transcriptional activity by stabilizing their interaction with TEA domain (TEAD) transcription factors (Peng et al., 2017). Of note, the metabolic shift from oxidative respiration to aerobic glycolysis is one of the classical hallmarks of cancer, suggesting that the increased glucose consumption that allows increased cell proliferation in cancer cells is besides sustaining the acquirement of tumorigenic features by promoting YAP/TAZ transcriptional program. This self-sustaining loop is supported by the effect that YAP/TAZ have on metabolism modifications, since they directly regulate transcription of glycolysis enzymes, HBP, and enzymes involved into glutamine metabolism and nucleotide biosynthesis (Nokin et al., 2016).

YAP/TAZ in mechanotransduction

Despite being at the nexus of a complex network of regulations as described above, YAP/TAZ function is, however, always influenced by a more basal level of regulation, represented by the integrity of the extracellular environment. Indeed YAP/TAZ role in the transduction of a broad range of mechanical signals into specific transcriptional program is essential in every process they mediate, either in healthy or in diseased tissues (reviewed in Panciera et al., 2017). Understanding how signals emanating from the extracellular environment are

integrated from mechanotransducers and then converted into cell-specific biological response is fundamental to fully appreciate cell behaviors in complex and spatio-temporal organized contexts as tissues and organs, and could be essential in the discovery of mechanisms that drive pathological states. Mechanotransduction defines the capability of cells to sense the physical inputs conveyed by the microenvironment, and to convert mechanical cues into biochemical signals to induce specific cellular responses (Halder et al., 2012). YAP/TAZ are the mediators of this signal transduction, and convert mechanical cues into specific transcriptional programs. Corruption of the cell niche is a primary cause of aberrant YAP/TAZ activation, that in turn leads to several diseases, such atherosclerosis, inflammation, muscular dystrophy and, importantly, cancer. YAP/TAZ activity is regulated by cell shape and polarity, but also by several topological cues, such as the conformation and the rigidity of the extracellular matrix (ECM) (Fig. 2B I). Indeed, cells plated on large and stiff substrates can spread and develop high cytoskeletal tension, mediated by ROCK and non-muscle-myosin-II, that ultimately results in YAP/TAZ activation (Fig. 2B II-III). Conversely, when cells are plated on softer or smaller adhesive substrates, the inability to develop sufficient cytoskeletal forces induces cytoplasmic retention and inhibition of YAP/TAZ. This mechanism offers the possibility to regulate YAP/TAZ activity in cells by experimentally reorganizing the F-actin cytoskeleton: depletion of Cofilin-1 and CapZ, F-actin capping and severing proteins, as well as F-actin stabilization by Phalloidin treatment, strongly induce YAP/TAZ transcriptional activity. On the contrary, treatment with toxins that inhibit F-actin polymerization, as Latrunculin A or Cytochalasin D, invariably result in YAP/TAZ inhibition (Aragona et al., 2013; Dupont et al., 2011). The fact that cell spreading involves F-actin cytoskeleton rearrangement, and in turn YAP/TAZ activity modulation, implies that also molecular components of focal adhesions (FAs), as integrins, focal adhesion kinase (FAK) and Src, are required for YAP/TAZ activity (Fig. 2B II-III). Moreover, the dynamic maturation of FAs is itself influenced by substrate stiffness, suggesting that FA components might not only be essential for cell-ECM adhesion, but can also be considered as mechanosensors (Hu et al., 2017; Taniguchi et al., 2015). It thus seems that YAP/TAZ regulation is not guided by the quantitative amount of F-actin, but rather by its organization, structure and tension. Of note, a considerable fraction of the YAP/TAZ transcriptional program is involved in a positive feedback loop to promote ECM proteins, integrins and FA docking protein transcription, promoting mechanical reciprocity between the cell and its

microenvironment (Martin et al., 2016; Morikawa et al., 2015). However, the mechanism that allows the propagation of signals transduced by the F-actin cytoskeleton into direct alterations of YAP/TAZ subcellular localization and activity is still unclear. One possibility that we considered in this work is that Angiomotin family proteins (AMOTs) could convey mechanical signals from F-actin structures to YAP/TAZ, since AMOTs bind YAP/TAZ, but can also interact with F-actin in a manner mutually exclusive with their YAP/TAZ association.

Hypotheses and aim

YAP/TAZ are key factors in the tumorigenic process, from early stages, in which they sustain the acquisition of cancer stem cell traits, to more advanced phases in which they foster tumor overgrowth by sustaining proliferation and angiogenesis. However, what are commonly considered the drivers of tumorigenesis are the so called oncogenic lesions, which are genetic alterations of tumor suppressor genes or proto-oncogenes overrepresented in different kinds of tumors. This kind of mutations usually correlate with proliferative advantage and the acquisition of the other classical hallmarks of cancer (Hanahan and Weinberg, 2011). However, what is still not completely defined even today, 30 years after the functional definition of an oncogenic mutation (Shih et al., 1979), is the identification of a common molecular mechanism accounting for the acquisition of the tumorigenic properties associated to oncogenic driver mutations. Intriguingly though, these cell behaviors are closely corresponding with those induced by hyperactivation of YAP/TAZ, as described above. Considering that YAP/TAZ are rarely bearing activating mutations in human malignancies, but, nevertheless, are often hyperactivated in either tumoral cells or tumor-associated stromal cells, we asked whether classical drivers of tumorigenesis could thus induce YAP/TAZ aberrant activation to promote malignant phenotypes. In this work, we focused on two different drivers of mutagenesis: mutant KRas and HER2. KRas activating mutations (G12D or G12V) are almost ubiquitously found in human PDAC cells, and are considered as driver mutations, since they have been detected in low grade PanINs and since oncogenic KRas expression is sufficient to induce PanIN lesions in mouse models (Ying et al., 2016). HER2 is one of the members of the family of epidermal growth factor receptor (EGFR). Gene amplification is responsible for increased expression of HER2 in almost 30% of sporadic breast cancer, and has been associated with poor clinical outcome (Marcotte and Muller, 2008). We initially asked if KRas and HER2 overexpression could specifically promote YAP/TAZ transcriptional activity in cell lines, and then we tested if oncogenic lesions require YAP/TAZ to promote initial transformation steps in primary pancreatic acinar cells and in mammary luminal differentiated cells. We also noted that both pancreatic adenocarcinoma and breast cancer are desmoplastic diseases, in which an aberrant tumor stroma is required to sustain uncontrolled proliferation of cells (Levental et al., 2009; Ying et al., 2016). As such, considering that the overall increased rigidity of the tumor can promote YAP/TAZ activation

by sustaining mechanotransduction, we asked whether interfering with the mechanotransduction pathway might prove to be an effective means to blunt the tumorigenic effect of YAP/TAZ downstream of oncogenic stimulation. In the last part of this work, we then investigated on the mechanism by which mechanical signals can be transduced to YAP/TAZ, and then converted into transcriptional programs that drive tumorigenic biological responses.

Results

YAP/TAZ are widespread hyperactivated in several solid tumors, being the mediators of several key features of cancer cells. For example, they promote aberrant proliferation, they are involved in drug resistance mechanisms, and mediate the capability to escape cell death programs. However, YAP/TAZ hyperactivation can never be ascribed to point mutations in their coding sequence, and only in rare types of malignancies amplifications or mutations in other components of their regulatory pathways are reported. On the other hand, several conserved genetic alterations are recurrently found in human tumors, targeting those that are, for this reason, referred to as oncogenes.

I) YAP/TAZ transcriptional activity is promoted by KRas and HER2 overexpression.

We started to ask if classical drivers of tumorigenesis could be able to activate YAP/TAZ and exploit them to foster tumor initiation. We decided to focus on two genetic alterations: KRas activating mutation (G12D), that is the driver mutation of most human pancreatic adenocarcinomas (Eser et al., 2014; Ying et al., 2016), and HER2 amplification, responsible for about one third of luminal breast cancers, that we recapitulated with a constitutive active mutant (V659E) (Marcotte and Muller, 2008). First of all, we tested the capability of oncogenic lesions to promote YAP/TAZ transcriptional activity. For this, we exploited luciferase reporters in which the luciferase coding sequence is expressed downstream of a synthetic promoter sequence recognized by TEAD factors, that are the binding platform of YAP/TAZ on DNA. This promoter sequence is thus bound only when YAP/TAZ are active in cells, serving as proxy for their transcriptional activity. To test whether YAP/TAZ activity could be stimulated by oncogene activation, we concomitantly transfected HEK293 cells with the YAP/TAZ-TEAD luciferase reporter and with increasing doses of plasmids expressing either mutant-KRas (pCS2-FLAG-KRas^{G12V}) (Fig 3A) or constitutive active-HER2 (pcDNA-HER2-V659E) (Fig. 3B) proteins. We observed that YAP/TAZ transcriptional activity is significantly increased by oncogene overexpression, and in a dose dependent manner, both in the case of KRas and in the case of HER2 hyperactivation. Since the luciferase reporter allows

to evaluate YAP/TAZ activation only indirectly, we verified the specificity of this result by repeating the experiment in HEK293 cells concomitantly depleted of YAP/TAZ by transfection with two independent mixes of siRNAs. As expected, YAP/TAZ depletion invariably resulted in a reduction in YAP/TAZ-TEAD reporter activation mediated by either KRas or HER2 overexpression (Fig 3A and 3B). By immunoblot analysis of the same cell lysates employed in the luciferase assay, we found that YAP/TAZ proteins are stabilized upon either KRas (Fig 3C) or HER2 (Fig 3D) overexpression. We thus asked whether the increase in YAP/TAZ protein levels could be due to a transcriptional regulation; for this, we measured *Yap* and *Taz* mRNA levels in HEK293 cells by qRT-PCR, finding that *Yap* and *Taz* relative mRNA expression is not affected by overexpression of KRas or HER2 (Fig 3E). This data thus suggested that oncogenes can activate YAP/TAZ through a post-translational mechanism of stabilization.

II) YAP/TAZ are mediators of the initial steps of tumorigenesis

Considering that oncogene overexpression can promote YAP/TAZ transcriptional activity in HEK293 cell lines, we asked to what extent YAP/TAZ might be required to promote tumor initiation downstream to the activation of oncogenic driver mutations. For this, we decided to study the effect of oncogenes in the cells of origin of tumors driven by KRas and HER2 alterations, that are respectively pancreatic acinar cells and luminal cells of the mammary gland.

II.II) YAP/TAZ are required for KRas mediated cell transformation of pancreatic acinar cells

To study the requirement of YAP/TAZ for the transformation of pancreatic acinar cells, we employed an experimental set up that allows to study the initial metaplastic event that leads to the development of Pancreatic Ductal Adenocarcinoma (PDAC) and permits to follow *ex vivo* the process of Acinar-to-Ductal Metaplasia (ADM) starting from freshly explanted primary acinar cells (Shi et al., 2013). In this set up primary acinar cells are isolated from the pancreas of adult *LSL-KRas*^{G12D} mice. The pure population of exocrine acinar cells obtained

after dissociation is then infected with an Adenoviral vector carrying the Cre recombinase (Ad-Cre), allowing the recombination of the LOX-STOP-LOX cassette, and thus permitting the expression of mutant KRas in acinar cells. Acini are then embedded in a three-dimensional collagen I-based matrix (experimental outline in Fig 4A). In few days of culture, acinar cells convert into ductal-like cells, that grow as spheroids in three dimensions, closely reminiscing the acinar-to-ductal metaplastic event observed *in vivo*. As comparison, *wt* cells prepared and cultured in the same fashion, invariably remain as non-proliferating acinar clusters until the experimental endpoint (Fig 4B). Interestingly, by immunofluorescence, we observed that cells that undergo KRas-driven ADM have a strong nuclear accumulation of YAP/TAZ when compare to *wt* acinar cells, that instead do not show any YAP/TAZ staining (Fig 4B). To test if such accumulation parallels with an increased YAP/TAZ activity, we analyzed by qRT-PCR the expression of two classical YAP/TAZ endogenous target genes: *Cyr61* and *CD44*. As shown in Fig 4C, KRas overexpression strongly induces YAP/TAZ transcriptional activity, measured by the upregulation of their specific targets. Since KRas overexpression is sufficient to activate YAP/TAZ in primary acinar cells, we next asked if YAP/TAZ are genetically required downstream of KRas for the process of cell transformation. To test this hypothesis, we repeated the acinar-to-ductal metaplasia experimental set up but changing the genetic background of acinar cells: we isolated cells from mice that express the *LSL-KRas^{G12D}* allele described above, but that also bear *Yap$^{fl/fl}$* and *Taz$^{fl/fl}$* alleles (Fig 5A). Once infected with Adenoviral Cre to activate KRas expression and concomitantly knock out both *Yap* and *Taz*, cells were seeded in collagen matrix to assess the formation of ductal-like structures. As shown in Fig 5B (and quantified in Fig 5C), YAP/TAZ depleted cells do not undergo ADM and remain as acinar clusters, just like *wt* cells. In line, we also observed that YAP/TAZ depletion impairs an intrinsic feature of the acinar to ductal change of fate, that is the acquired proliferation capability. Indeed, ductal-like cells are positive for Ki67 staining, a marker of proliferation, while cells that are YAP/TAZ depleted are completely growth arrested (Fig 5D), despite the expression of mutant KRas. This suggested a strict YAP/TAZ requirement downstream of KRas to allow acinar-to-ductal transition. We thus next moved to test YAP/TAZ requirement *in vivo* in a mouse model of pancreatic cancer, that allows to study early genetic events at the tumor onset. We employed mice bearing the *LSL-KRas^{G12D}* allele alone, or in combination with *Yap$^{fl/fl}$* and *Taz$^{fl/fl}$* alleles. Mice also express a tamoxifen-inducible Cre^{ERTM} recombinase expressed downstream of the *Ptf1a* promoter, that is active

only in exocrine acinar cells in adult mice, and that allows KRas STOP cassette removal and concomitant *Yap* and *Taz* depletion in a tightly space and time controlled manner. Mice with KRas mutation in acinar cells develop ADM, ultimately resulting in the emergence of observable PanINs six months after induction of the oncogene by intraperitoneal (I.P.) tamoxifen injection (Fig 5E). Strikingly, in mice in which KRas mutant is expressed in cells concomitantly depleted of YAP/TAZ, ADM events are almost completely abolished (Fig 5E and 5F). Data presented so far demonstrated that KRas overexpression promotes YAP/TAZ transcriptional activity, and that this activation is required to promote initial tumorigenic event in the pancreas.

II.III) YAP/TAZ mediates cell plasticity conferred by HER2 overexpression in mammary gland luminal cells

Since we found that promotion of YAP/TAZ activity downstream of oncogenic drivers is not exclusive of KRas, but is recapitulated also by HER hyperactivation (see Fig. 3), we decided to assess the requirement of YAP/TAZ downstream of HER2 overexpression in primary luminal cells of the mammary gland. We chose this model as HER2 amplification is one of the most common driver mutations observed in breast cancer, account for more than 25% of all mammary tumors. For this, we looked again at the earlier events of tumorigenic transformation, that entail the acquirement of progenitor-like proliferating capacity by terminally differentiated mammary luminal cells. We thus exploited an experimental set up that allows to discriminate if terminally differentiated primary cells acquire the capability to grow in a clonogenic medium, that is a property specific of progenitor cells (Panciera et al., 2016). We isolated primary luminal cells from *wt* mice by Fluorescence Activated Cell Sorting (FACS). Epithelial cells are first sorted as lineage negative (Lin^-) and EpCAM positive epithelial cells, and then separated into three different populations using CD49f and CD61 as surface markers (Guo et al., 2012). Different populations are respectively enriched in mammary gland stem cells (MaSC) ($EpCAM^{low}$, $CD61^+$, $CD49f^{high}$); Luminal Progenitors cells (LP) ($EpCAM^{high}$, $CD61^+$, $CD49f^{low}$) and Luminal Differentiated cells (LD) ($EpCAM^{high}$, $CD61^-$, $CD49f^{low}$) (Fig 6A). We decided thus to investigate the effect of HER2 overexpression and on the possibility that this could induce a change of fate in differentiated

primary cells, mimicking the initial cell plasticity event occurring in transformed cells (experimental outline in Fig 6B). Cells were plated on collagen I-coated wells and infected with lentiviral vectors encoding constitutive active HER2 downstream of a doxycycline-dependent promoter (FuTetO-HER2-V659E) and the TetOn promoter transactivator element (FuDeltaGW-rtTA). After 24 hours from infection, cells were treated with doxycycline to induce HER2 overexpression. After 7 days from induction, the same number of LD and LP cells expressing HER2 or control vector (FuTetO-empty), and MaSC cells was seeded in a clonogenic medium containing 5% of Matrigel and doxycycline to sustain HER2 expression (Fig 6B). As shown in Fig 6C, only luminal cells (LD and LP) expressing HER2 could form colonies, similar to the ones originated from Mammary Stem Cells, while control luminal cells invariably remain as single cells embedded in the medium. HER2 overexpression also confers the capability to self-renew, since colonies originated from either LD or LP cells infected with HER2 could be passaged, after dissociation and replating, giving rise to secondary and tertiary colonies with the same self-renewing capacity of endogenous MaSCs (quantified in Fig 6D). Of note after 7 days of induction, colonies can grow also in absence of doxycycline (-DOXY) at passaging. This was likely due to the capacity of HER2 to induce endogenous YAP activation, which is the promoter of self-renewal. Indeed, as described in Panciera et al., 2016, a transient exogenous stimulation is sufficient to stably promote endogenous YAP hyperactivation, and thus to sustain progenitor-like features without the need of continuous overexpression of exogenous YAP, or, in this case, HER2. The capability to form self-renewing colonies can be considered as a hallmark of a change of fate that primary differentiated cells undergo upon HER2 overexpression, recapitulating the initial event that leads to tumor development *in vivo*.

As we did in the model of plasticity induced by mutant KRas in pancreatic cells, we asked whether YAP/TAZ could play a central role in the change of fate from luminal differentiated cells to mammary progenitor-like cells. To assess YAP/TAZ requirement we repeated the above experiment isolating cells from mammary glands of mice bearing $Yap^{fl/fl}$ and $Taz^{fl/fl}$ alleles. Cells were purified and treated as described above, but adding Adenoviral vectors carrying Cre recombinase or GFP control sequences (Ad-Cre or Ad-GFP) to allow *Yap* and *Taz* knock out (Fig 7A). After 15 days in clonogenic medium we looked for the presence of colonies, that were able to grow only from LD and LP cells expressing HER2, while cells lacking YAP/TAZ remained as single cells, similarly to control cells (Fig 7B and 7C), despite

HER2 overexpression. This demonstrates that YAP/TAZ are required downstream of HER2 to mediated luminal cells transformation.

III) Targeting mechanotransduction as a strategy to inhibit oncogene mediated YAP/TAZ activation

In the experiments described so far, we identified YAP/TAZ as common mediators of the tumorigenic properties conferred by two different oncogenic lesions: KRas mutation and HER2 hyperactivation. YAP/TAZ are often inconsequential for the normal homeostasis of adult tissues, and in particular in the case of pancreas and mammary gland, where they are instead involved respectively in the processes of tissue regeneration and ductal expansion during pregnancy and lactation (Chen et al., 2014). As we showed, YAP/TAZ are also absolutely required for tumorigenic onset in these same tissues. For this reason, we surmised that YAP/TAZ could be considered as specific target for anti-cancer therapies. In this line, we asked how to inhibit YAP/TAZ in order to curb the effect of oncogene activation. Among several pathways that impinge on YAP/TAZ activity, as outlined in introduction, mechanotransduction is increasingly recognized as the basal layer of YAP/TAZ regulation. This means that a certain amount of mechanical strain is always necessary in order to allow YAP/TAZ nuclear accumulation. We decided thus to interfere with this pathway to study if lowering mechanical stimulation sensed by cells could be sufficient to inhibit YAP/TAZ activation downstream of oncogenic signaling in primary cells. Of note, desmoplastic stroma that normally surrounds cancer cells is often stiffer than normal, further indicating the overall altered tumoral mechanical environment as a promoting factor for malignant phenotypes (Bissell and Hines, 2011; Butcher et al., 2009).

III.I) KRas tumorigenic effect relies on YAP/TAZ mechanotransduction

We started by asking whether interfering with the micro-environmental stiffness could affect KRas-driven metaplasia of primary pancreatic acinar cells. The experimental set up we employed to study KRas effect in pancreatic acini was perfectly suitable for this purpose,

since it allows to directly observe the effect of the oncogene on explanted cells embedded in a reconstituted extracellular matrix. In this case, however, we sought to embed acinar cells in matrices of different rigidity, to study the effect of the extracellular environment in mutant KRas acinar cells. We achieved this technical improvement by employing a Poly (ethylene glycol) acrylate hydrogel, based on a four-arm PEG polymer, used as building block, that allows for precise control of the three-dimensional matrix stiffness by modulating the amount of crosslinker peptides, that covalently bind PEG polymers though a UV-mediated Michael addition reaction. These matrices were rendered biocompatible by also adding RGD-containing peptides, that allow cell-matrix adhesion by mimicking the integrin-bound RGD fragment of fibronectin (Arg-Gly-Asp) (Fig 8A and 8B, and experimental procedures section).

We isolated pancreatic acinar cells carrying the *LSL-KRas*^{G12D} allele, and once we induced KRas overexpression by Ad-Cre infection, we seeded cells in matrices of different rigidity. As shown in Fig 8C, only acinar cells embedded in hydrogels stiffer than 1 kPa can undergo ADM, while cells in softer extracellular environments remain as acinar clusters. Interestingly, there is a threshold of rigidity below which oncogene is completely ineffective, but above this threshold, extracellular rigidity seems to impact on KRas effect in a sort of dose-dependent fashion: the number of ADM event increases in parallel with the progressive stiffening of the hydrogel (Fig 8D). This experiment suggests that oncogenes require a minimal proficient mechanotransduction to work, and that the efficiency of the oncogene in inducing ADM depends on the amount of mechanical stress that cells experience.

To further confirm the hypothesis that cells need to efficiently transduce mechanical inputs to sustain KRas effect, we decided to interfere with mechanotransduction by impinging on the pathway from the intracellular side, that is by affecting the integrity of the F-actin cytoskeleton. We thus treated cells with two different drugs: Latrunculin A (LatA), that binds monomeric actin preventing filament polymerization, and Cytochalasin D (CytoD), that interacts with the ends of actin filaments, blocking elongation. Both drugs cause, in the end, aberrant cytoskeletal assembly and, at high doses, morphological alterations of cells. Of note, both these drugs are well characterized as YAP/TAZ mechano-inhibitors (Dupont et al., 2011). We embedded *wt* or *KRas*-mutant acini in collagen I-based matrix, and we treated cells with two different doses of LatA and CytoD. Treated cells were not able to undergo ADM, despite the overexpression of the oncogene (Fig 8E and 8F), confirming that KRas is unable

to promote cell transformations in cells in which mechanical signals are insufficient to sustain YAP/TAZ activity.

III.II) YAP/TAZ as therapeutic target to inhibit KRas mediated tumorigenesis

We next asked if the inhibitory mechanism described above could be exploited in a pre-clinical perspective, to inhibit tumor initiation. To answer this question, we decided to employ two different drugs that impair a proper cytoskeletal assembly, as described in the previous experiment, but that are under evaluation in clinical trials or already approved for patient treatment. The first one is Defactinib, an inhibitor of Focal Adhesion Kinase (FAK). FAK activates the signaling cascade that is downstream of integrin clustering occurring for example when cells are on stiff substrates. The second one is Dasatinib, employed as chemotherapic agent in different types of leukemias. Among other tyrosin kinases, it is an inhibitor of Src kinases family, that is another focal adhesion associated kinase. Both drugs inhibit the propagation of the signal that is initially stimulating an integrin-mediated response, that in turn activates focal adhesion-associated kinases and their downstream signaling cascade. Of note, several proteins of this mechano-sensory apparatus, have already been reported as YAP/TAZ regulators (Hu et al., 2017; Taniguchi et al., 2015). To test their efficacy in inhibiting KRas tumorigenic activity, we isolated cells from mice carrying *LSL-KRas*^{G12D}, we embedded acini in collagen I matrix and we treated cells by adding Defactinib or Dasatinib to the culture medium. Again, only untreated cells were efficiently transformed by KRas overexpression, while drug treatment resulted in a very efficient inhibition of ADM (Fig 9A and 9B). To prove that the effect of inhibition of focal adhesion could be ascribed to YAP/TAZ inhibition, we tried to elude the inhibitory effect of Defactinib and Dasatinib by overexpressing YAP. We isolated acinar cells from a mouse model bearing KRas mutation and a tetracycline dependent operator that drives the inducible overexpression of a hyperactive form of YAP (TetO-YAP^{S127A}). To allow YAP expression, mice also carry an optimized reverse tetracycline transactivator cloned into the ROSA26 locus (R26-rtTAM2). Acini were embedded in collagen I and treated with doxycycline to concomitantly activate the expression of KRas and YAP. As shown in Fig 9A and 9B, KRas alone is not sufficient to induce ADM in acinar cells treated with Defactinib or Dasatininb, but providing robust expression of an exogenous YAP renders cells able to transform also in conditions in which

normally endogenous YAP, even when induced by KRas, is inhibited by insufficient mechanical stimulation. This correlates well with the observation that by immunofluorescent staining, YAP/TAZ are activated and nuclearly localized in KRas-induced ductal-like structure, but completely absent in cells treated with Defactinib and Dasatinib (Fig 9C).

IV) Soft extracellular matrix inhibits tumor growth *in vivo*

So far, we demonstrated that oncogenes can efficiently induce malignant phenotypes in primary cells through YAP/TAZ activation, but only in cells that can sustain YAP/TAZ nuclear accumulation through functional mechano-signaling. However, the experiments we did to demonstrate our hypothesis were all made manipulating primary cells *ex vivo*, in models that recapitulate an initial event of cell plasticity. We thus decided to test the effect of mechanical alterations *in vivo*, in murine models of breast cancer and pancreatic adenocarcinoma.

IV.I) Lysyl Oxydase inhibitor blunts tumor overgrowth in a mammary carcinoma mouse model

To study whether mechanical manipulation could affect mammary carcinoma formation *in vivo,* we employed mice carrying the MMTV-PyMT allele, that allows expression of Polyoma Middle T antigen driven by the promoter of the Mouse Mammary tumor virus. These mice develop aggressive carcinomas already at 7-8 weeks of age. MMTV-PyMT induced tumors that strongly resemble luminal carcinomas induced by HER2 activated by the same MMTV promoter (Herschkowitz et al., 2007). It is reported that carcinomas are often desmoplastic diseases, and in particular collagen I deposition and organization have been related to tumor progression. Of note, mammographic density is indeed a prominent diagnostic marker employed for the detection of breast cancer nodules. We thus decided to reduce tumor extracellular environment rigidity by treating mice with an inhibitor of Lysyl Oxydase (LOX), an enzyme that initiates the process of covalent collagen crosslinking. LOX inhibition is known to reduce tissue stiffness and to prevent fibrosis, and the LOX inhibitor BAPN (beta-aminopropionitrile) has already been used to inhibit breast cancer progression in a similar set-up (Levental et al., 2009). We treated MMTV-PyMT mice by administrating BAPN in

drinking water, for 8 weeks, starting from the fourth week of age (experimental outline in Fig 10A), until experimental humane endpoint. Mammary gland phenotypes were then analyzed through different kind of staining of tissue sections (Fig 10B). Hematoxylin-Eosin staining of mammary gland sections showed that MMTV-PyMT mice invariably develop carcinomas. However, the huge carcinomas that invade MMTV-PyMT tissue are strongly reduced by BAPN treatment, almost reminiscing a control *wt* tissue. To control the efficacy of the treatment we visualized extracellular collagen fibers with Picrosirius red staining, and indeed the thick collagen fibers network enmeshed into the tumoral mass is reduced almost to normal levels by LOX inhibition. Interestingly, even the small neoplastic formations that are still present after BAPN treatment, show a dramatically lowered rate of proliferation, as shown in Fig 10B by Ki67 immunohistochemistry (IHC). Most importantly, YAP IHC staining revealed that cells of the cancerous mass have strong YAP nuclear staining, that is completely lost upon BAPN treatment (Fig 10B), even in the residual small neoplastic formations, indicating that matrix softening strongly affects YAP/TAZ nuclear accumulation also *in vivo,* and that this mechanism curbs tumor growth.

IV.II) Lysyl Oxidase inhibitor treatment reduces progression of Pancreatic Adenocarcinoma in vivo

To further confirm the efficacy of reducing tissue stiffening to inhibit tumorigenic effect of oncogenes, we decided to test the efficacy of BAPN treatment also in a mouse model of pancreatic adenocarcinoma. The experiment was designed to investigate if the overall stiffness of the extracellular environment could be considered as a therapeutic target to inhibit tumor overgrowth, also considering that, in particular in PDAC, rigidity is a peculiar feature of the tumor itself (Cannon et al., 2018). The genetic model we chose for this experiment allowed us to analyze the effect of KRas overexpression in acinar cells (as in the experiment described in Fig 5E) through Ptf1a-Cre^{ERTM}, LSL-KRas^{G12D} alleles, with the additional expression of an inducible mutant p53 allele (p53-LSL-R172H) in the same cells. Mutant p53 promotes PDAC faster onset and progression, allowing a shorter experimental outcome. Mice were treated with tamoxifen by intraperitoneal injection at 4 weeks of age, to induce Cre^{ERTM} mediated activation of KRas and p53 mutant alleles. At 5 weeks of age we started to treat

mice with BAPN, administered in drinking water. Mice were kept under BAPN treatment for 12 weeks, at the endpoint pancreata were collected and stained for different markers (Experimental outline in Fig 11A). By Hematoxylin-Eosin staining we assessed the presence of huge PDACs growing in pancreata of KRas and p53 mutant mice, that were dramatically inhibited upon BAPN treatment. As we did in the mammary gland analogous experiment, we visualized collagen fibers by Picrosirius Red staining, that revealed a massive amount of stromal deposition into the PDAC masses. Extracellular collagen deposition in pancreas of mice treated with BAPN was comparable to control mice, confirming the efficacy of the treatment. Interestingly, PDAC cells show great accumulation of nuclear YAP and TAZ, while acinar cell of the pancreas of treated mice do not express YAP/TAZ, closely resembling healthy control acini (Fig 11B). This experiment, in parallel with the one we carried out in MMTV-PyMT mice, confirmed that tumor extracellular environment is crucial to sustain the progression of cancer, and demonstrated that removal of the mechanical strain that support YAP/TAZ activity in cancer cells is sufficient to blunt tumor overgrowth.

V) Members of the Angiomotin protein family are YAP/TAZ mechano-regulators

Data presented so far show that the physical extracellular environment has a central role in instructing cell behavior, inducing reactions that start as signaling cascades activated upon integrin clustering, are propagated into the cell through cytoskeletal modification, and are finally converted into biochemical signals that are conveyed to the nucleus. YAP/TAZ are nuclear transducers of this pathway, and we demonstrated that also their well-known role in tumorigenesis is conditioned by this basal and widespread level of regulation. However, despite the huge impact that mechanical strains exert on cells, either in physiological or in pathological conditions, the mechanism responsible for direct YAP/TAZ regulation downstream of different physical inputs has not been fully defined yet. We know that in conditions in which cells can develop several interactions with the extracellular matrix (as on stiff substrates), integrins cluster and induce the activation of Focal Adhesion associated kinases, that in turn promote stress fiber polymerization and contractility (Panciera et al., 2017). This process ultimately activates YAP/TAZ, but which is the factor that can convey information from F-actin status to YAP/TAZ remains unknown. We reasoned that a family

of protein that have already been reported as YAP/TAZ inhibitor, Angiomotin proteins, is a promising candidate for such a role. The motin family is composed by three members: AMOT130, AMOTL1 and AMOTL2. All these proteins can directly interact with YAP and TAZ via L/PPXY motif, mostly through YAP and TAZ WW domain (Moleirinho et al., 2014). Interesting, motins can also bind F-actin, and this interaction involves the same motin protein region that is engaged in YAP/TAZ interaction (Mana-Capelli et al., 2014). For this, a model can be envisioned in which motins interact with YAP and with F-actin in a mutually exclusive manner. We thus asked if Angiomotin interaction with F-actin could affect their negative regulation of YAP/TAZ, and, in other words, if motins could behave as YAP/TAZ inhibitors in response to different mechanical conditions.

V.I) Angiomotins behave as YAP/TAZ inhibitors in classical mechano-assays

To test the effect of motins in cells subjected to different mechanical stimulations, we set-up a luciferase assay to analyze YAP/TAZ transcriptional activity (through the same YAP/TAZ-TEAD promoter used in experiments in Fig 3), in HEK293T cells plated in different mechanical conditions. For this we employed classical mechano-assays that have been employed to modulate YAP/TAZ activity: we know that YAP/TAZ are nuclear and active in cells plated on stiff substrates (>5-10 kPa), as on polystyrene plates, and when cells are plated at low confluence. On the other hand, YAP/TAZ are cytoplasmic and inactive in cells plated on soft substrates (as poly-acrylamide gels with elastic modulus lower than 1,5 kPa, for epithelial cells) or when they are plated at high confluence (Aragona et al., 2013; Panciera et al., 2017). We first tested the effect of the depletion of all Angiomotin members, achieved by transfection of two independent mixes of siRNAs. As shown in Fig 12A, YAP/TAZ transcriptional activity, that is blunted in cells plated on soft poly-acrylamide substrates, is efficiently rescued by motins depletion to levels comparable to the cells plated on stiff substrate. On the other hand, upon overexpression of AMOT by plasmid transfection, YAP/TAZ transcriptional activity in HEK293T cells plated at low confluence dramatically drops to levels even lower than in cells at high confluence, in which YAP/TAZ are cytoplasmic and inactive (Fig 12B). We also evaluated YAP/TAZ subcellular localization, as visualized by immunofluorescent staining, and we observed that, in HEK293T cells at high

confluence, in which YAP is retained in the cytoplasm, Angiomotin proteins depletion shifts YAP localization into the nucleus, as if cells were plated at low confluence (Fig 12C, quantification of average subcellular localization in Fig 12D).

V.II) Angiomotins inhibit YAP/TAZ in response to cytoskeletal modifications

Experiments described so far suggested that Angiomotin proteins could have an inhibitory role on YAP/TAZ, that is more evident in conditions of low mechanical stress, since motins depletions in cells plated on soft substrate or at high confluence is sufficient to rescue YAP/TAZ transcriptional activity. Starting from this observation, and from the reported mutually exclusive interaction between Angiomotins and YAP/TAZ, we hypothesized the mechanism by which YAP/TAZ are inhibited in cells experiencing low mechanical stresses. We surmised that in cells that are able to stretch, and that have a highly polymerized and contractile cytoskeleton, motins are mostly bound to F-actin fibers and only a low fraction might interact with YAP/TAZ, inhibiting their nuclear accumulation. On the contrary, in cells that are experiencing low mechanical stress, in which F-actin is less polymerized, an increased fraction of Angiomotins might be released from the interaction with F-actin, and be free to bind YAP/TAZ, with a resulting increased inhibitory effect (scheme in Fig 13A). To validate this mechanism, we first analyzed AMOT differential interaction with F-actin. We performed differential lysates of HEK293T cells by the use of a low detergent hypotonic buffer that allows to separate two different subcellular fractions: one contains F-actin and its interactors (insoluble fraction, Ins.) and the other contains soluble proteins that are free from F-actin interaction (soluble fraction, Sol.). We analyzed lysates by immunoblot to assess AMOT protein levels. In control cells, two different subpools of AMOT exist: one is bound to F-actin and one is free in the soluble fraction. But interestingly, treatment with Phalloidin, a toxin that binds F-actin preventing its de-polymerization, and that thus mimics a condition of high mechanical stress, induces AMOT complete re-localization into the insoluble, F-actin bound fraction (Fig 13B). This experiment confirms that motins interaction with the cytoskeleton is quantitative, and depends on the level of polymerization of F-actin. To better understand if this behavior could actually affect Angiomotins capability to inhibit YAP/TAZ, we analyzed their interaction by a co-immunoprecipitation experiment in which we exploited endogenous YAP as bait to immune-precipitate endogenous AMOT in HEK293T cells. In control cells

we validated the interaction, since YAP immunoprecipitated AMOT (compare lane 1 with 3 and 4 of Fig 13C). F-actin stabilization, by Phalloidin treatment, strongly reduced AMOT binding to YAP (Fig 13C, compare lanes 1 and 2), confirming that variations in AMOT binding to F-actin directly affect AMOT capability to inhibit YAP, and, in other words, that the mutually exclusive binding of Angiomotins to the cytoskeleton or to YAP/TAZ is actually the mechanism that allows YAP/TAZ regulation in response to cytoskeletal alterations.

Conclusions

YAP/TAZ are activated downstream of oncogenic lesions

Tumor cells often bear recurrent genetic alterations, that are responsible for the loss of function of tumor suppressor genes or for the activation of proto-oncogenes. These alterations are considered as drivers of tumorigenesis, but a common molecular player responsible for the activation of the transcriptional programs involved in cell malignant transformation has never been identified. On the other hand, YAP/TAZ are known to be the promoters of several features associated to malignant phenotypes. We thus hypothesized that the different pathways activated downstream of oncogenes could converge on YAP/TAZ activation. In this work, we found that two of the most common genetic alterations, namely mutant KRas and HER2, can promote YAP/TAZ transcriptional activity, by stabilizing YAP and TAZ proteins. This initial observation sustained the hypothesis by which YAP/TAZ could be recruited downstream of the activation of oncogenes, raising interest towards YAP/TAZ as the nuclear determinants of oncogene-mediated transformation. Of note, despite the consistent efforts devoted to develop molecularly targeted agents for patient-specific therapies, a substantial improvement in the survival rate is still lacking (Le Tourneau et al., 2015). This suggests that despite the identification of oncogenic lesions as drivers of tumorigenesis, efficient targeted therapies might need to consider molecular targets more generally required to foster tumorigenic properties. In this scenario, the identification of a common factor activated by different drivers of tumorigenesis might offer a new avenue for therapeutic exploitation.

Oncogenes hijack YAP/TAZ activity to initiate tumorigenesis

Tumorigenesis is a complex and multi-step process that is scarcely amenable to investigate *in vitro*, but dissecting early events of cell transformation might be essential to identify the molecular players of the tumorigenic process, and likely to identify possible therapeutic targets. In this work, we exploited experimental settings that allow to assess the effect of oncogenes in primary pancreatic acinar cells and in primary luminal differentiated cells of the mammary gland. This allowed us to demonstrate that overexpression of KRas and HER2 induce cell plasticity in primary differentiated cells, that acquire progenitor-like properties and start proliferating. This observation correlates with recent discoveries on the cell of origin

of cancer, showing that often these are not somatic stem cells that simply enter in an uncontrolled loop of proliferation, but adult differentiated cells that undergo de-differentiation upon oncogenic stimulation (Feng et al., 2014; Friedmann-Morvinski et al., 2012; Kopp et al., 2012; Van Keymeulen et al., 2015). In particular, it was demonstrated that pancreatic cancer cells, that show ductal-like features, actually originate from acinar cells that undergo Acinar-to-Ductal Metaplasia (ADM) (Kopp et al., 2012). Similarly, oncogenic stimulation in mammary gland luminal cells activates a multipotent genetic program in lineage-restricted populations to promote tumor initiation (Van Keymeulen et al., 2015). Interestingly, a previous work done in our laboratory demonstrated that YAP/TAZ overexpression is sufficient to promote cell plasticity, reprogramming adult differentiated cells into their lineage specific somatic stem cells (Panciera et al., 2016). This evidence, together with the discovery that oncogenes promote cell plasticity as initial event of the tumorigenic process, reinforced the hypothesis by which YAP/TAZ are activated downstream of oncogenes to mediate the biological responses that are at the core of tumorigenesis. In line, we demonstrated that oncogenes rely on YAP/TAZ activation to promote cell plasticity in primary cells. This was confirmed also *in vivo*, in a mouse model of pancreatic adenocarcinoma, in which tumor initiation and growth was completely blunted by depleting YAP/TAZ in a mutant KRas genetic background.

YAP/TAZ mechanotransduction modulates oncogene-mediated tumorigenesis

Once we demonstrated the requirement of YAP/TAZ downstream of oncogenes overexpression we decided to target these factors to inhibit tumorigenesis induced by oncogenic lesions. Considering that tumors are often desmoplastic diseases in which aberrant deposition of stroma sustains YAP/TAZ activity, and considering that mechanotransduction pathway is known to be a primary means of YAP/TAZ regulation, we decided to interfere with mechanical signaling to inhibit YAP/TAZ and thus tumor overgrowth. We confirmed that a proficient propagation of the mechanical cues from the extracellular environment is necessary to sustain YAP/TAZ even when these are hyperactivated by oncogenes. Indeed, we were able to inhibit KRas-induced Acinar-to-Ductal Metaplasia by mechano-inhibiting YAP/TAZ. Interestingly the same inhibitory effect was obtained by softening the extracellular environment, that is from an outward point of view, and by rendering cells unable to transduce the signal by interfering with the F-actin cytoskeleton integrity, and thus from the inner side

of the cell. This evidence suggested that even if YAP/TAZ are necessary downstream of oncogenic stimulation to foster tumorigenesis, oncogenes alone are not sufficient to induce the initial metaplastic events that eventually lead to tumor formation. Indeed, a minimal threshold level of YAP/TAZ activation has to be granted to induce cell transformation. This means that extracellular environment and genetic background must cooperate to sustain YAP/TAZ tumorigenic transcriptional programs. Of note, this reflects well with the notion that from a purely genetic standpoint, cancer develops with a surprising relative low incidence compared to the high rate of mutations that are expected in the trillions of cells that compose the human body (Bissell and Hines, 2011). We thus envision a scenario in which extracellular environment is protective, with its capacity to balance aberrant cell behaviors, but can become a tumor promoting factor when its composition and physical attributes are aberrantly altered, in cases such as chronic pancreatitis for pancreatic cancers, or fibrosis and inflammation. The notion by which tumor growth needs at least one "initiator" and one or more "promoters" was put forward since in the 1980s (Slaga, 1983); however today an efficient strategy to hit cancer from different fronts is still missing. For this we reasoned that addressing a "tumor-supportive" factor, as an over-reactive stroma, might be a promising therapeutic perspective, as suggested by our finding that clinically actionable drugs such as Defactinib and Dasatinib to inhibit KRas-induced ADM. Targeting YAP/TAZ in tumor cells could be an efficient strategy to blunting tumor overgrowth without the risk of an excessive toxicity, since YAP/TAZ are often inconsequential for adult tissue homeostasis (Azzolin et al., 2014; Cai et al., 2015; Chen et al., 2014; Zanconato et al., 2015). Targeting mechanotransduction to YAP/TAZ is a highly promising strategy in this direction, as proven by the massive tumor-inhibitory effect that we observed by impairing the stromal stiffening both of PDAC and of mammary carcinoma when we treated mice the lysyl oxidase inhibitor BAPN.

Angiomotins: novel hints in the YAP/TAZ mechanotransduction pathway

In the last part of this work we addressed what is still a major black box in the mechanotrasduction field, that is the mechanism responsible for the transduction of mechanical cues from the F-actin cytoskeleton, which is rearranged in response to extracellular stimulation, to YAP/TAZ regulation. We demonstrated that Angiomotin proteins are potent YAP/TAZ inhibitors, and that their effect on YAP/TAZ is modulated by F-acting rearrangement, suggesting that Angiomotins might be the direct YAP/TAZ

mechano-inhibitors. From a mechanistic standpoint, we found that Angiomotins inhibit YAP/TAZ by direct binding, and that this binding is mutually exclusive to Angiomotin binding to F-actin. As such, in mechanically stimulated cells an increase in F-actin deposition diverts Angiomotins from YAP/TAZ, in this way allowing for YAP/TAZ activation. This finding uncovers a fundamental player in the mechanostransduction pathway to YAP/TAZ.

Experimental procedures

The methods here listed are part of the Piccolo lab protocol book and are thus presented with minor modifications, if any, in respect to any material published by our laboratory.

Reagents and plasmids

FBS, L-Glutamine, Pen/Strep (10,000 U/mL), DMEM medium, Waymouth's medium Trypsin-EDTA 0,05%, ITS-X, BPE supplement were from Life Technologies. BAPN, DMSO, BSA, SBTI, dexamethasone, doxycycline hyclate, Rat Tail Collagen I (coating), Phoshatase Inhibitor Cocktail 2, Dithiothreitohl, Adenosine 5'-Triphosphate disodium salt hydrate, Latrunculin A, Cytochalasin D were from Sigma. Complete Mini, EDTA-Free was from Roche. Matrigel Growth Factor Reduced Basement Membrane Matrix, Phenol Red-Free was from Corning. Rat Tail Collagen I for 3D culture was from Cultrex. Recombinant FGF10, Noggin, EGF, bFGF were from Peprotech. Defactinib and Dasatinib were from Selleckchem. 4 Arm PEG-acrylate (MW 20K) was from JenKem Technology USA. Custom crosslinker peptide was from Caslo. Custom RDG peptide was from SynPeptide. Lithium Phenyl(2,4,6-trimethylbenzoyl)phosphinate (initiator) was from Tokio Chemical Industry.

Cre- and GFP-expressing adenoviruses were from University of Iowa, Gene Transfer Vector Core.

pCDNA3-HER2-CA V659E (# 16259), FUdeltaGW-rtTA (#19780), FUW-tetO-MCS (#84008), pCDNA3-HA-AMOT p130 (#32821) were from Addgene. pCS2-FLAG-KRas-G12V was subcloned from pBABE-KRas G12V (Addgene #46746), FUW-tetO-HER2-CA V659E was subcloned from pCDNA3-HER2-CA V659E. pRL-TK (renilla) is from Promega. 8xGTIIC–LUX and CTGF-LUX (YAP/TAZ-TEAD reporters) were previously described respectively in Dupont et al., 2011 and Zanconato et al., 2015.

Cell lines and transfection

HEK293 and HEK293T cells were from ATCC. Both were cultured in DMEM supplemented with 10%FBS, 2mM L-Glutamine and Pen/Strep.

siRNA transfections were performed using Lipofectamine RNAiMAX (Life technologies) in antibiotics-free medium (Opti-MEM Medium, Gibco), according to manufacturer instructions. Cells were seeded to be 30% confluent at the time of transfection.

DNA transfections were done with TransIT-LT1 (Mirus Bio) according to manufacturer instructions. Cells were seeded to be at 50% at the time of transfection.

siRNAs sequences used are:

siControl (siAS)	AllStars Negative Control siRNA 1027280 (Qiagen)
siYAP#1	CUGGUCAGAGAUACUUCUU
siYAP#2	GACAUCUUCUGGUCAGAGA
siTAZ#1	AGGUACUUCCUCAAUCACA
siTAZ#2	ACGUUGACUUAGGAACUUU
siAMOT	CACCAACGTTTCAGAATACAA
siAMOTL1	CAACGAGGAACTGCCCACTTA
siAMOTL2#1	CTGTATGTTTAAGTTATCGTA
siAMOTL2#2	AAACTAGTTAATGAGCTACAA

Mixes were composed as following: mix siYAP/TAZ#1 contains siYAP#1 and siTAZ#1 in equimolar ratio, mix siYAP/TAZ#2 contains siYAP#2 and siTAZ#2 in equimolar ratio, mix siAMOTS A contains siAMOT, siAMOTL1 and siAMOTL2#1 in equimolar ratio, mix siAMOTS A contains siAMOT, siAMOTL1 and siAMOTL2#2 in equimolar ratio.

Lentiviral preparation

HEK293T cells were kept in DMEM supplemented with 10% FBS (Life Technologies), Glutamine and Antibiotics. Lentiviral particles were prepared by transiently transfecting HEK293T with lentiviral vectors (10 micrograms/10 cm dishes) together with packaging vectors pMD2-VSVG (2.5 micrograms) and pPAX2 (7.5 micrograms) by using TransIT-LT1 (Mirus Bio) according to manufacturer instructions. Specifically, 60 µl of TransIT-LT1 reagent was diluted in 1.5 ml of Opti-MEM (Life Technologies) for each 10 cm dish, incubated with the vector DNA 15 min at RT and gently distributed over to the cell medium (dish contained about 10 ml of HEK medium). After 8 hr, HEK medium was changed. 48 hr

post-transfection supernatant was collected, filtered through 0.45 micrometers and directly stored at -20°C; we did not concentrate viral supernatants.

Mice

Animal experiments were performed adhering to our institutional guidelines (CEASA, Comitato Etico per la Sperimentazione Animale, corresponding to our Animal Welfare Body).

Wt CD1 mice are from Charles river. *Ptf1a-CRE^{ER}* mice (stock #019378) and *MMTV-PyMT* mice (stock #001800) were purchased from The Jackson Laboratory, *LSL-KRasG12D* mice were received from T. Jacks, *p53 LSL-R172H* mice were received from G. Lozano, *Yap1$^{fl/fl}$* mice were provided by D. Pan, *Taz$^{fl/fl}$* mice were described in Azzolin et al., 2014., *TetO-YAPS127A* were received from F. Camargo.

Primary pancreatic acinar cells isolation and culture

Primary pancreatic acini were isolated from the pancreas of 6- to 9-week-old mice, as described in (Panciera et al., 2018). Digested tissue was filtered through a 100 μm nylon cell strainer. The quality of isolated acinar tissue was checked under the microscope. For culture of entire acini, explants were seeded in neutralized rat tail collagen type I (Cultrex)/acinar culture medium (1:1), overlaid with acinar culture medium (Waymouth's medium supplemented with 0.1% FBS, 0.1% BSA, 0.2 mg/ml SBTI, 1x ITS-X, 50 μg/ml BPE, 1μg/ml dexamethasone, and antibiotics) once collagen formed a gel. ADM events were assessed 5 days after seeding. To activate KRas overexpression, acinar cells were infected with Ad-Cre for 3 hours at 37°C before seeding. To induce YAP^{S127A} expression cells were cultured in the presence of 2 μg/ml doxycycline.

For the experiment described in Fig. 8C-D, a PEG-based mixture was prepared as following: PEG 4-arm and initiator were separately resuspended in PBS 1X. RGD and crosslinker peptides were separately resuspended in H2O pH 5,5 and then pH was further adjusted to 5,5. In particular, crosslinker peptide was resuspended at different concentrations, to confer different specific rigidity to the hydrogel after polymerization. Then initiator and the two peptides are added in this order to PEG suspension. Acinar cells are then resuspended in the final mixture, seeded and quickly exposed to UV light (600 sec at 15mV cm^2) by using a Delolux 20 UV lamp of 400 nm wavelength.

Mammary luminal cells isolation and culture

Primary mammary cells were isolated from the mammary glands of 8- to 12-week-old virgin mice, as described in Panciera et al., 2018.

Briefly, mammary glands were minced and digested before sorting. To separate various subpopulations cells were stained for 30 min at 4°C with antibodies against CD49f (PE-Cy5, cat. 551129, BD Biosciences), CD29 (PE-Cy7, cat. 102222, BioLegend), CD61 (PE, cat. 553347, BD Biosciences), EpCAM (FITC, cat. 118208, BioLegend) and lineage markers (APC mouse Lineage Antibody Cocktail, cat. 51-9003632, BD Biosciences) in DMEM/F12.

The stained cells were then resuspended in PBS/BSA 0,1% and sorted on a BD FACS Aria sorter (BD Biosciences) into luminal differentiated (LD) cells, luminal progenitor (LP) cells and mammary stem cells (MaSCs).

After FACS purification, cells were seeded in collagen-I coated 24-well plates and infected with lentiviral vectors (virus suspension was mixed 1:1 with medium) or with Ad-Cre/Ad-GFP, and eventually treated with doxycycline for 7 days. After one week, mammary cells were detached with trypsin and seeded at a density of 2000 cells/well in 24-well ultralow attachment plates (Corning) in mammary clonogenic suspension medium (DMEM/F12 containing glutamine, antibiotics, 5% Matrigel, 5% FBS, 10 ng/ml murine EGF, 20 ng/ml murine bFGF, and 4 μg/ml heparin) containing doxycycline (2 μg/ml). Primary colonies were counted 14 days after seeding. To show the self-renewal capacity of primary colonies, these were recovered from the clonogenic medium by collecting and incubating cell suspensions with an excess volume of ice cold HBSS in order to solubilize Matrigel. After 1 hour, colonies were rinsed 3 times in cold HBSS by centrifugation at 1000 rpm for 5 min and incubated in trypsin 0.05% for 30 min to obtain a single cell suspension. Cells were counted and re-seeded at 2000 cells/well in 24-well ultralow attachment plates in mammary clonogenic suspension medium.

Luciferase assay

YAP/TAZ-TEAD reporters (8xGTIIC–LUX or CTGF-LUX, 100ng) were transfected into HEK293 or HEK293T cells seeded in 3,9 cm^2 multiwell plates, together with increasing doses of pCDNA3-HER2-CA V659E or pCS2-FLAG-KRas-G12V or with pCDNA3-HA-

AMOT p130 (250ng) and TK-Renilla (100ng) to normalize for transfection efficiency. DNA content in all samples was kept uniform by adding pBluescript plasmid up to 1 μg. In experiments described in Fig 3 cells were transfected with siRNAs 24 hours after plating, and transfected with plasmids 48 hours after plating. Cells were then harvested 24 hours after plasmid transfection. In experiments described in Fig. 12A cells were transfected with siRNAs 24 hours after plating, transfected with plasmids 48 hours after plating and replated onto different substrates 24 hours after plasmid transfection. In experiments described in Fig. 12B cells were transfected with plasmids 24 hours after plating, and replated at different confluences 24 hours after plasmid transfection. Cells were then harvested 24 hours after replating. Firefly and *Renilla* luciferase activity was measured with an Infinite F200PRO plate reader (TECAN). Data are presented as firefly/*Renilla* luciferase activity.

Immunoblot

Immunoblots were carried out as described in Cordenonsi et al.,2011. Anti-YAP/TAZ (63.7; sc-101199) and anti-AMOT (B-4; sc-166924) monoclonal antibodies were from Santa Cruz. Anti-betaActin (A5316) was from Sigma. Anti-GAPDH (MAB347) mouse monoclonal antibody was from Millipore. Secondary anti-mouse-HRP was from GE-Healthcare.

Co-immunoprecipitation of endogenous proteins

For immunoprecipitation of endogenous proteins, HEK293T cells were transfected with siRNAs as indicated. Cells were treated with Phalloidin (50μM) for 4 hours before harvesting. Cells were collected 24 hours after transfection. Cell lysis and immunoprecipitation were performed in mild hypotonic buffer (35μl/cm^2, 20mM Hepes, 50mM KCl, 0,1% NP40, 0;1% Triton X-100, 5% glycerol, 5mM$MgCl_2$, phospatase inhibitor, protease inhibitor, DTT 1mM, ATP 1mM, proteasome inhibitor, creatinine phosphate 10μM). To immuno-precipitate endogenous YAP, anti-YAP (13584-1-AP, Proteintech) was bound to ProteinA-Dynabeads (Invitrogen) and incubated with cell lysates at 4°C overnight, all diluted in lysis buffer corrected to optimize immune-precipitation efficiency. Resulting binding buffer was obtained by adding to lysis buffer: 100mM NaCl, 1,5 mM MgCl2, 0,2 mM EDTA, 15% glycerol.

Differential actin extracts

HEK293T cells were plated at 40% confluence, transfected with siRNAs as indicated, and eventually treated with Phalloidin for 4 hours before lysis. Cells were incubated for 3 minutes with warm mild hypotonic buffer (35µl/cm^2, 20mM Hepes, 50mM KCl, 0,1% NP40, 0;1% Triton X-100, 5% glycerol, 5mMMgCl_2, phospatase inhibitor, protease inhibitor, DTT 1mM, ATP 1mM, proteasome inhibitor, creatinine phosphate 10µM) to obtain the soluble fraction. Further 10 µl/cm^2 of buffer were added to the plate, the remaining insoluble fraction was scraped and collected. Both fractions were mechanically lysed with a syringe, and centrifuged to pellet cell debris. Supernatants were collected, quantified and treated as standard immunoblot samples as described in Cordenonsi et al., 2011.

RNA extraction, reverse transcription and quantitative real-time PCR

Total RNA was extracted using RNeasy Mini Kit (Qiagen) according to manufacturer instructions. Before cDNA synthesis, the samples were quantified using NanoDrop 2000c Spectrophotometer (Thermo scientific). 1µg of RNA for each sample was heated for 5 minutes at 70 °C to denature the secondary structures. The retrotranscription reaction mix contains FS buffer, 10 mM DTT, 2 mM dNTPs mix, 25 ng oligo-d(T), 100U Mo-MLV ReverseTranscriptase (Invitrogen), 40U RNAseOUT Recombinant RNAse Inhibitor (Invitrogen). Reactions were incubated at 37 °C for one hour and half, then at 70 °C for 10 minutes to inactivate the enzyme.

Quantitative real-time PCR (qPCR) analyses were carried out on cDNAs with Rotor-Gene Q (Qiagen) thermal cycler. Every amplification reaction contained: cDNA, 0.5 µM each primer (see table below for primer sequences), and FastStart SYBR Green Master (Roche). Amplification was carried out as follows: 10 seconds at 95 °C, 15 seconds at 60 °C, 20 seconds at 72 °C for 40 cycles. Each sample was run in triplicate; expression values of target genes were normalized to *Gapdh* or *18S rRNA* expression.

gene	Forward primer sequence	Reverse primer sequence
hGapdh	ATCCTGCACCACCAACTGCT	GGGCCATCCACAGTCTTCTG
hYAP1	GCACCTCTGTGTTTTAAGGGTCT	CAACTTTTGCCCTCCTCCAA
hTAZ	GGCTGGGAGATGACCTTCAC	CTGAGTGGGGTGGTTCTGCT
m18S rRNA	TGTCTCAAAGATTAAGCCATGC	GCGACCAAAGGAACCATAAC
mCyr61	GCTCAGTCAGAAGGCAGACC	GTTCTTGGGGACCAGAGGA
mCD44	CTCCTGGCACTGGCTCTGAT	CAGATTCCGGGTCTCGTCAG

Immunofluorescence, staining and microscopy

For immunofluorescence on cells, these were fixed in PFA 4% for 10 minutes, after washing with PBS cells were permeabilized 10 min at RT with PBS 0.3% Triton X-100, and processed for immunofluorescence using the following conditions: blocking in 10% Goat Serum (GS, Invitrogen) in PBS 0.1% Triton X-100 (PBST) for 1 hour followed by incubation with primary antibodies (diluted in 2% GS in PBST) overnight at 4°C, four washes in PBST and incubation with secondary antibodies (1:200 in 2% GS in PBST) for 2 hours at room temperature. Samples were mounted with ProLong-DAPI (Molecular Probes, Life Technologies) that allows to label cell nuclei.

For immunofluorescence on pancreatic acini, pancreatic acini were fixed overnight in PBS 4% PFA at 4°C, permeabilized with two washes in PBS 0.5% NP40 for 20 minutes at 4°C, followed by one wash in PBS 0.3% Triton X-100 for 20 minutes at room temperature. After two washes in PBS 0.1% Triton X-100 (PBST) for 15 minutes at room temperature, acini were blocked with two washes in PBST 10% GS for 1 hour at room temperature, and incubated overnight with primary antibodies. The following day, cells were washed twice in PBST 2% GS for 15 minutes at 4°C, and five more times in PBST 2% GS for 1 hour at 4°C. Secondary antibodies were incubated overnight. The third day, cells were washed five times in PBST for 15 minutes, incubated 20 min with DAPI solution and mounted in glycerol.

Primary antibodies used: Anti-YAP/TAZ (63.7; sc-101199), anti-Ki67 (SpringBio). Alexa-conjugated secondary antibodies (Life Technologies): Alexa-Fluor-488 donkey anti-mouse IgG (A21202), Alexa Fluor-488 donkey anti-rabbit IgG (A21206), Alexa-Fluor-568-Phalloidin (A12380).

Confocal images were obtained with a Leica TCS SP5 equipped with a CCD camera.

Immunohistochemical staining was performed on formalin-fixed, paraffin-embedded mammary gland and pancreas sections as described in Cordenonsi et al., 2011. Anti-Ki67 polyclonal antibody (clone SP6; M3062) was from Spring Bioscience; anti-YAP (13584-I-AP, Proteintech), anti-TAZ (anti-WWTR1, HPA007415) was from Sigma.

PicroSirius Red staining was performed according to manufacturer procedures (Polysciences Inc.).

References

Aragona, M., Panciera, T., Manfrin, A., Giulitti, S., Michielin, F., Elvassore, N., Dupont, S., and Piccolo, S. (2013). A Mechanical Checkpoint Controls Multicellular Growth through YAP/TAZ Regulation by Actin-Processing Factors. Cell *154*, 1047–1059.

Azzolin, L., Zanconato, F., Bresolin, S., Forcato, M., Basso, G., Bicciato, S., Cordenonsi, M., and Piccolo, S. (2012). Role of TAZ as Mediator of Wnt Signaling. Cell *151*, 1443–1456.

Azzolin, L., Panciera, T., Soligo, S., Enzo, E., Bicciato, S., Dupont, S., Bresolin, S., Frasson, C., Basso, G., Guzzardo, V., et al. (2014). YAP/TAZ Incorporation in the β-Catenin Destruction Complex Orchestrates the Wnt Response. Cell *158*, 157–170.

Bartucci, M., Dattilo, R., Moriconi, C., Pagliuca, A., Mottolese, M., Federici, G., Benedetto, A.D., Todaro, M., Stassi, G., Sperati, F., et al. (2015). TAZ is required for metastatic activity and chemoresistance of breast cancer stem cells. Oncogene *34*, 681–690.

Bissell, M.J., and Hines, W.C. (2011). Why don't we get more cancer? A proposed role of the microenvironment in restraining cancer progression. Nat. Med. *17*, 320–329.

Brusatin, G., Panciera, T., Gandin, A., Citron, A., and Piccolo, S. (2018). Biomaterials and engineered microenvironments to control YAP/TAZ-dependent cell behaviour. Nat. Mater. *17*, 1063–1075.

Butcher, D.T., Alliston, T., and Weaver, V.M. (2009). A tense situation: forcing tumour progression. Nat. Rev. Cancer *9*, 108–122.

Cai, J., Maitra, A., Anders, R.A., Taketo, M.M., and Pan, D. (2015). β-Catenin destruction complex-independent regulation of Hippo–YAP signaling by APC in intestinal tumorigenesis. Genes Dev. *29*, 1493–1506.

Calvo, F., Ege, N., Grande-Garcia, A., Hooper, S., Jenkins, R.P., Chaudhry, S.I., Harrington, K., Williamson, P., Moeendarbary, E., Charras, G., et al. (2013). Mechanotransduction and YAP-dependent matrix remodelling is required for the generation and maintenance of cancer-associated fibroblasts. Nat. Cell Biol. *15*, 637–646.

Camargo, F.D., Gokhale, S., Johnnidis, J.B., Fu, D., Bell, G.W., Jaenisch, R., and Brummelkamp, T.R. (2007). YAP1 Increases Organ Size and Expands Undifferentiated Progenitor Cells. Curr. Biol. *17*, 2054–2060.

Chen, Q., Zhang, N., Gray, R.S., Li, H., Ewald, A.J., Zahnow, C.A., and Pan, D. (2014). A temporal requirement for Hippo signaling in mammary gland differentiation, growth, and

tumorigenesis. Genes Dev. *28*, 432–437.

Cordenonsi, M., Zanconato, F., Azzolin, L., Forcato, M., Rosato, A., Frasson, C., Inui, M., Montagner, M., Parenti, A.R., Poletti, A., et al. (2011). The Hippo Transducer TAZ Confers Cancer Stem Cell-Related Traits on Breast Cancer Cells. Cell *147*, 759–772.

Diep, C.H., Zucker, K.M., Hostetter, G., Watanabe, A., Hu, C., Munoz, R.M., Von Hoff, D.D., and Han, H. (2012). Down-Regulation of Yes Associated Protein 1 Expression Reduces Cell Proliferation and Clonogenicity of Pancreatic Cancer Cells. PLoS ONE *7*, e32783.

Dupont, S., Morsut, L., Aragona, M., Enzo, E., Giulitti, S., Cordenonsi, M., Zanconato, F., Le Digabel, J., Forcato, M., Bicciato, S., et al. (2011). Role of YAP/TAZ in mechanotransduction. Nature *474*, 179–183.

Enzo, E., Santinon, G., Pocaterra, A., Aragona, M., Bresolin, S., Forcato, M., Grifoni, D., Pession, A., Zanconato, F., Guzzo, G., et al. (2015). Aerobic glycolysis tunes YAP/TAZ transcriptional activity. EMBO J. *34*, 1349–1370.

Eser, S., Schnieke, A., Schneider, G., and Saur, D. (2014). Oncogenic KRAS signalling in pancreatic cancer. Br. J. Cancer *111*, 817–822.

Feng, X., Degese, M.S., Iglesias-Bartolome, R., Vaque, J.P., Molinolo, A.A., Rodrigues, M., Zaidi, M.R., Ksander, B.R., Merlino, G., Sodhi, A., et al. (2014). Hippo-Independent Activation of YAP by the GNAQ Uveal Melanoma Oncogene through a Trio-Regulated Rho GTPase Signaling Circuitry. Cancer Cell *25*, 831–845.

Friedmann-Morvinski, D., Bushong, E.A., Ke, E., Soda, Y., Marumoto, T., Singer, O., Ellisman, M.H., and Verma, I.M. (2012). Dedifferentiation of Neurons and Astrocytes by Oncogenes Can Induce Gliomas in Mice. Science *338*, 1080–1084.

Guo, W., Keckesova, Z., Donaher, J.L., Shibue, T., Tischler, V., Reinhardt, F., Itzkovitz, S., Noske, A., Zürrer-Härdi, U., Bell, G., et al. (2012). Slug and Sox9 Cooperatively Determine the Mammary Stem Cell State. Cell *148*, 1015–1028.

Halder, G., Dupont, S., and Piccolo, S. (2012). Transduction of mechanical and cytoskeletal cues by YAP and TAZ. Nat. Rev. Mol. Cell Biol. *13*, 591–600.

Hanahan, D., and Weinberg, R.A. (2011). Hallmarks of Cancer: The Next Generation. Cell *144*, 646–674.

Harvey, K.F., Pfleger, C.M., and Hariharan, I.K. (2003). The Drosophila Mst Ortholog, hippo, Restricts Growth and Cell Proliferation and Promotes Apoptosis. Cell *114*, 457–467.

Herschkowitz, J.I., Simin, K., Weigman, V.J., Mikaelian, I., Usary, J., Hu, Z., Rasmussen,

K.E., Jones, L.P., Assefnia, S., Chandrasekharan, S., et al. (2007). Identification of conserved gene expression features between murine mammary carcinoma models and human breast tumors. Genome Biol. *8*, R76.

Hu, J.K.-H., Du, W., Shelton, S.J., Oldham, M.C., DiPersio, C.M., and Klein, O.D. (2017). An FAK-YAP-mTOR Signaling Axis Regulates Stem Cell-Based Tissue Renewal in Mice. Cell Stem Cell *21*, 91-106.e6.

Kopp, J.L., von Figura, G., Mayes, E., Liu, F.-F., Dubois, C.L., Morris, J.P., Pan, F.C., Akiyama, H., Wright, C.V.E., Jensen, K., et al. (2012). Identification of Sox9-Dependent Acinar-to-Ductal Reprogramming as the Principal Mechanism for Initiation of Pancreatic Ductal Adenocarcinoma. Cancer Cell *22*, 737–750.

Le Tourneau, C., Delord, J.-P., Gonçalves, A., Gavoille, C., Dubot, C., Isambert, N., Campone, M., Trédan, O., Massiani, M.-A., Mauborgne, C., et al. (2015). Molecularly targeted therapy based on tumour molecular profiling versus conventional therapy for advanced cancer (SHIVA): a multicentre, open-label, proof-of-concept, randomised, controlled phase 2 trial. Lancet Oncol. *16*, 1324–1334.

Levental, K.R., Yu, H., Kass, L., Lakins, J.N., Egeblad, M., Erler, J.T., Fong, S.F.T., Csiszar, K., Giaccia, A., Weninger, W., et al. (2009). Matrix Crosslinking Forces Tumor Progression by Enhancing Integrin Signaling. Cell *139*, 891–906.

Liang, N., Zhang, C., Dill, P., Panasyuk, G., Pion, D., Koka, V., Gallazzini, M., Olson, E.N., Lam, H., Henske, E.P., et al. (2014). Regulation of YAP by mTOR and autophagy reveals a therapeutic target of tuberous sclerosis complex. J. Exp. Med. *211*, 2249–2263.

Mana-Capelli, S., Paramasivam, M., Dutta, S., and McCollum, D. (2014). Angiomotins link F-actin architecture to Hippo pathway signaling. Mol. Biol. Cell *25*, 1676–1685.

Marcotte, R., and Muller, W.J. (2008). Signal Transduction in Transgenic Mouse Models of Human Breast Cancer—Implications for Human Breast Cancer. J. Mammary Gland Biol. Neoplasia *13*, 323–335.

Martin, K., Pritchett, J., Llewellyn, J., Mullan, A.F., Athwal, V.S., Dobie, R., Harvey, E., Zeef, L., Farrow, S., Streuli, C., et al. (2016). PAK proteins and YAP-1 signalling downstream of integrin beta-1 in myofibroblasts promote liver fibrosis. Nat. Commun. *7*, 12502.

Moleirinho, S., Guerrant, W., and Kissil, J.L. (2014). The Angiomotins – From discovery to function. FEBS Lett. *588*, 2693–2703.

Morikawa, Y., Zhang, M., Heallen, T., Leach, J., Tao, G., Xiao, Y., Bai, Y., Li, W., Willerson,

J.T., and Martin, J.F. (2015). Actin cytoskeletal remodeling with protrusion formation is essential for heart regeneration in Hippo-deficient mice. Sci. Signal. *8*, ra41–ra41.

Morvaridi, S., Dhall, D., Greene, M.I., Pandol, S.J., and Wang, Q. (2015). Role of YAP and TAZ in pancreatic ductal adenocarcinoma and in stellate cells associated with cancer and chronic pancreatitis. Sci. Rep. *5*.

Nokin, M.-J., Durieux, F., Peixoto, P., Chiavarina, B., Peulen, O., Blomme, A., Turtoi, A., Costanza, B., Smargiasso, N., Baiwir, D., et al. (2016). Methylglyoxal, a glycolysis side-product, induces Hsp90 glycation and YAP-mediated tumor growth and metastasis. ELife *5*.

Panciera, T., Azzolin, L., Fujimura, A., Di Biagio, D., Frasson, C., Bresolin, S., Soligo, S., Basso, G., Bicciato, S., Rosato, A., et al. (2016). Induction of Expandable Tissue-Specific Stem/Progenitor Cells through Transient Expression of YAP/TAZ. Cell Stem Cell *19*, 725–737.

Panciera, T., Azzolin, L., Cordenonsi, M., and Piccolo, S. (2017). Mechanobiology of YAP and TAZ in physiology and disease. Nat. Rev. Mol. Cell Biol. *18*, 758–770.

Panciera, T., Azzolin, L., Di Biagio, D., Totaro, A., Cordenonsi, M., and Piccolo, S. (2018). De Novo Generation of Somatic Stem Cells by YAP/TAZ. J. Vis. Exp.

Peng, C. Regulation of the Hippo-YAP Pathway by Glucose Sensor O-GlcNAcylation.

Ren, F., Zhang, L., and Jiang, J. (2010). Hippo signaling regulates Yorkie nuclear localization and activity through 14-3-3 dependent and independent mechanisms. Dev. Biol. *337*, 303–312.

Rosenbluh, J., Nijhawan, D., Cox, A.G., Li, X., Neal, J.T., Schafer, E.J., Zack, T.I., Wang, X., Tsherniak, A., Schinzel, A.C., et al. (2012). β-Catenin-Driven Cancers Require a YAP1 Transcriptional Complex for Survival and Tumorigenesis. Cell *151*, 1457–1473.

Serrano, I., McDonald, P.C., Lock, F., Muller, W.J., and Dedhar, S. (2013). Inactivation of the Hippo tumour suppressor pathway by integrin-linked kinase. Nat. Commun. *4*.

Shi, G., DiRenzo, D., Qu, C., Barney, D., Miley, D., and Konieczny, S.F. (2013). Maintenance of acinar cell organization is critical to preventing Kras-induced acinar-ductal metaplasia. Oncogene *32*, 1950–1958.

Slaga, T.J. Overview of Tumor Promotion in Animals. 12.

Song, Q., Mao, B., Cheng, J., Gao, Y., Jiang, K., Chen, J., Yuan, Z., and Meng, S. (2015). YAP Enhances Autophagic Flux to Promote Breast Cancer Cell Survival in Response to Nutrient Deprivation. PLOS ONE *10*, e0120790.

Sorrentino, G., Ruggeri, N., Specchia, V., Cordenonsi, M., Mano, M., Dupont, S., Manfrin, A., Ingallina, E., Sommaggio, R., Piazza, S., et al. (2014). Metabolic control of YAP and TAZ by the mevalonate pathway. Nat. Cell Biol. *16*, 357–366.

Taniguchi, K., Wu, L.-W., Grivennikov, S.I., de Jong, P.R., Lian, I., Yu, F.-X., Wang, K., Ho, S.B., Boland, B.S., Chang, J.T., et al. (2015). A gp130–Src–YAP module links inflammation to epithelial regeneration. Nature *519*, 57–62.

Totaro, A., Panciera, T., and Piccolo, S. (2018). YAP/TAZ upstream signals and downstream responses. Nat. Cell Biol. *20*, 888–899.

Van Keymeulen, A., Lee, M.Y., Ousset, M., Brohée, S., Rorive, S., Giraddi, R.R., Wuidart, A., Bouvencourt, G., Dubois, C., Salmon, I., et al. (2015). Reactivation of multipotency by oncogenic PIK3CA induces breast tumour heterogeneity. Nature *525*, 119–123.

Wada, K.-I., Itoga, K., Okano, T., Yonemura, S., and Sasaki, H. (2011). Hippo pathway regulation by cell morphology and stress fibers. Development *138*, 3907–3914.

Yin, F., Yu, J., Zheng, Y., Chen, Q., Zhang, N., and Pan, D. (2013). Spatial Organization of Hippo Signaling at the Plasma Membrane Mediated by the Tumor Suppressor Merlin/NF2. Cell *154*, 1342–1355.

Ying, H., Dey, P., Yao, W., Kimmelman, A.C., Draetta, G.F., Maitra, A., and DePinho, R.A. (2016). Genetics and biology of pancreatic ductal adenocarcinoma. Genes Dev. *30*, 355–385.

Yui, S., Azzolin, L., Maimets, M., Pedersen, M.T., Fordham, R.P., Hansen, S.L., Larsen, H.L., Guiu, J., Alves, M.R.P., Rundsten, C.F., et al. (2018). YAP/TAZ-Dependent Reprogramming of Colonic Epithelium Links ECM Remodeling to Tissue Regeneration. Cell Stem Cell *22*, 35-49.e7.

Zanconato, F., Forcato, M., Battilana, G., Azzolin, L., Quaranta, E., Bodega, B., Rosato, A., Bicciato, S., Cordenonsi, M., and Piccolo, S. (2015). Genome-wide association between YAP/TAZ/TEAD and AP-1 at enhancers drives oncogenic growth. Nat. Cell Biol. *17*, 1218–1227.

Zanconato, F., Cordenonsi, M., and Piccolo, S. (2016). YAP/TAZ at the Roots of Cancer. Cancer Cell *29*, 783–803.

Zhang, W., Nandakumar, N., Shi, Y., Manzano, M., Smith, A., Graham, G., Gupta, S., Vietsch, E.E., Laughlin, S.Z., Wadhwa, M., et al. (2014). Downstream of Mutant KRAS, the Transcription Regulator YAP Is Essential for Neoplastic Progression to Pancreatic Ductal Adenocarcinoma. Sci. Signal. *7*, ra42–ra42.

Zhao, B., Ye, X., Yu, J., Li, L., Li, W., Li, S., Yu, J., Lin, J.D., Wang, C.-Y., Chinnaiyan, A.M., et al. (2008). TEAD mediates YAP-dependent gene induction and growth control. Genes Dev. *22*, 1962–1971.

Zhao, B., Li, L., Wang, L., Wang, C.-Y., Yu, J., and Guan, K.-L. (2012). Cell detachment activates the Hippo pathway via cytoskeleton reorganization to induce anoikis. Genes Dev. *26*, 54–68.

(2018). Desmoplasia in pancreatic ductal adenocarcinoma: insight into pathological function and therapeutic potential. Genes Cancer.

Figures

Figure 1: YAP/TAZ in human solid malignancies

Graphical representation of human solid tumors for which YAP/TAZ activation has been reported to be relevant for malignant phenotypes.
Modified from Zanconato et al., 2016.

FIGURE 1

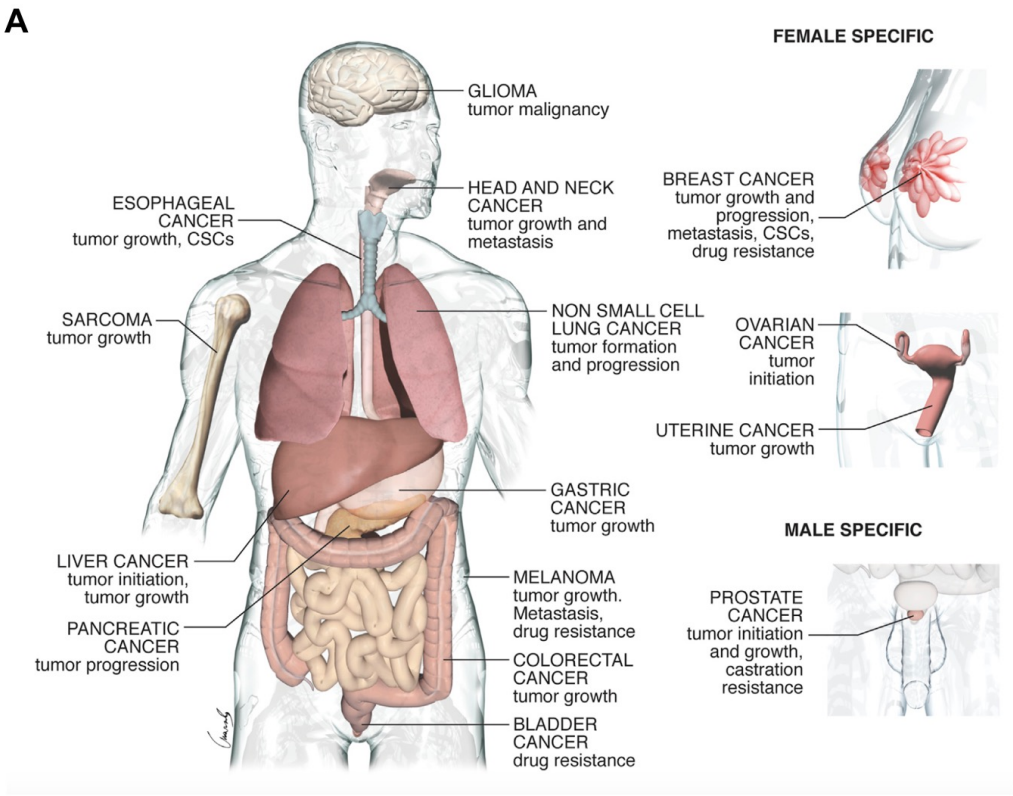
A
FEMALE SPECIFIC
GLIOMA
tumor malignancy
HEAD AND NECK
CANCER
tumor growth and
metastasis
ESOPHAGEAL
CANCER
tumor growth, CSCs
BREAST CANCER
tumor growth and
progression,
metastasis, CSCs,
drug resistance
SARCOMA
tumor growth
NON SMALL CELL
LUNG CANCER
tumor formation
and progression
OVARIAN
CANCER
tumor
initiation
UTERINE CANCER
tumor growth
GASTRIC
CANCER
tumor growth
MALE SPECIFIC
LIVER CANCER
tumor initiation,
tumor growth
MELANOMA
tumor growth.
Metastasis,
drug resistance
PROSTATE
CANCER
tumor initiation
and growth,
castration
resistance
PANCREATIC
CANCER
tumor progression
COLORECTAL
CANCER
tumor growth
BLADDER
CANCER
drug resistance

Figure 2: Malignant phenotypes and YAP/TAZ mechanotransdution

A: Schematic representation of the contribution of YAP/TAZ mechanotransduction in tumor growth. Tumor growth is associated with an enhanced activity of YAP in cancer-associated fibroblasts (CAFs) due to a stiffening of the extracellular matrix. YAP sustains the activity of CAFs and promotes collagen deposition and thus further stiffening of the ECM. Stiff ECM in turn promotes YAP/TAZ mechanotransduction to foster growth of tumor cells, acquisition of chemoresistance and metastatic dissemination. This mechanically activated positive loop results in a progressive worsening of the pathological outcome (Calvo et al., 2013; Halder et al., 2012; Panciera et al., 2017).

B: Schematic representation the signaling pathways that convey mechanical and physical cueas to YAP/TAZ. Integrin clustering activates focal-adhesion-associated kinases, such as focal adhesion kinase (FAK) and SRC, in response to stiff substrates. This pathway in turn favors stress fibers growth, stability and contractility and thus results in YAP/TAZ activation. RHO GTPases are also activated downstream of focal adhesion formation, and directly activate actin-regulatory proteins, such as actin-related protein 2/3 complex (ARP2/3) and Wiskott–Aldrich syndrome protein (WASP), or promote F-actin polymerization through RHO-associated protein kinase (ROCK); ROCK in turn promotes actomyosin contractility and activates LIM domain kinase (LIMK), an inhibitor of the F-actin-severing protein cofilin. In II and III, chemical inhibitors of different players in the YAP and TAZ mechanotransduction pathway are highlighted in grey (Aragona et al., 2013; Dupont et al., 2011; Sorrentino et al., 2014).

Modified from Panciera et al., 2017.

FIGURE 2

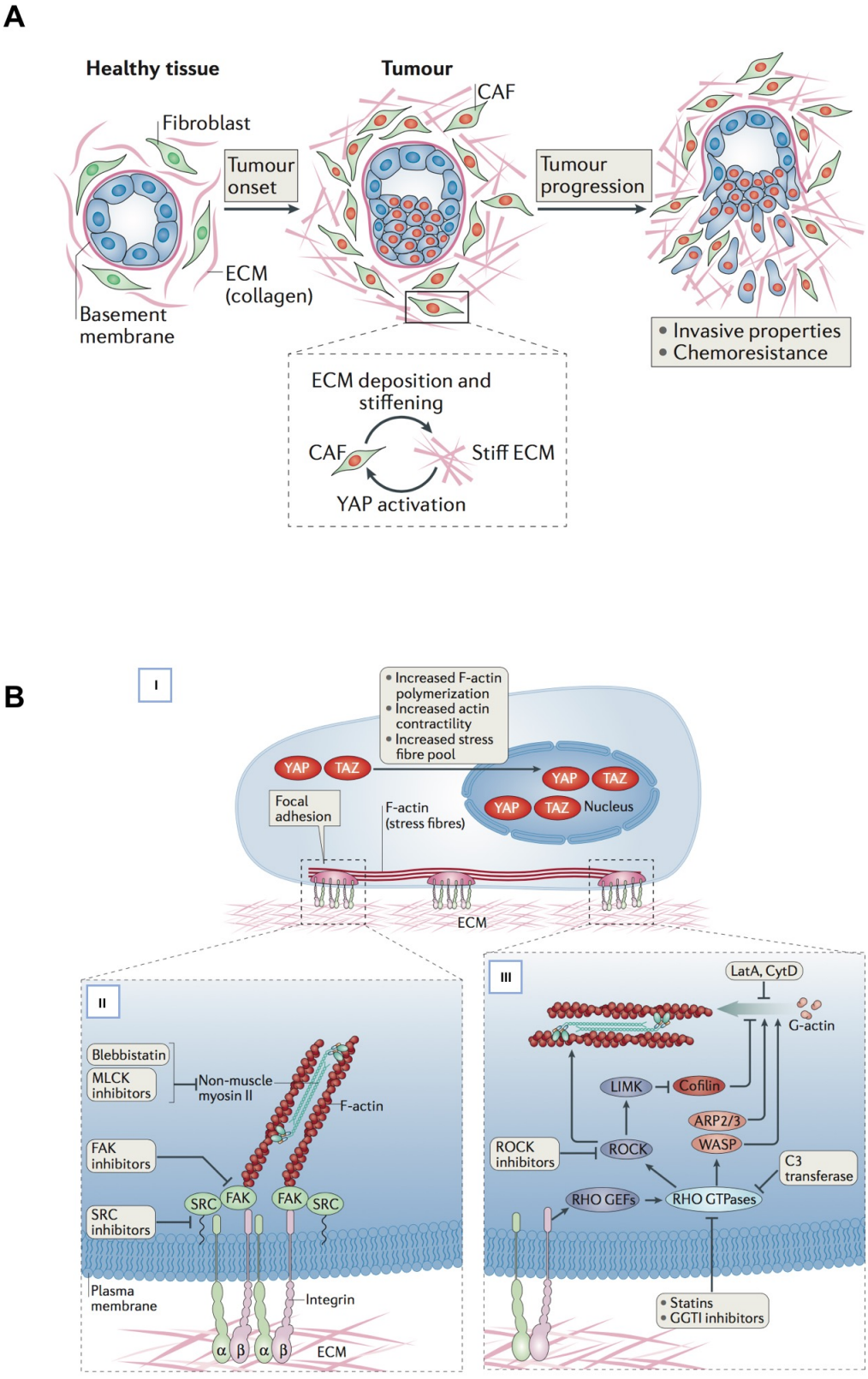
A
Healthy tissue
Tumour
Fibroblast
CAF
Tumour onset
Tumour progression
ECM (collagen)
Basement membrane
• Invasive properties
• Chemoresistance
ECM deposition and stiffening
CAF
Stiff ECM
YAP activation
B
I
• Increased F-actin polymerization
• Increased actin contractility
• Increased stress fibre pool
YAP
TAZ
Nucleus
Focal adhesion
F-actin (stress fibres)
ECM
II
Blebbistatin
MLCK inhibitors
Non-muscle myosin II
F-actin
FAK inhibitors
SRC
FAK
SRC inhibitors
Plasma membrane
Integrin
α β α β
ECM
III
LatA, CytD
G-actin
LIMK
Cofilin
ARP2/3
WASP
ROCK inhibitors
ROCK
C3 transferase
RHO GEFs
RHO GTPases
• Statins
• GGTI inhibitors

Figure 3: YAP/TAZ transcriptional activity is promoted by KRas and HER2 overexpression

A-B: Luciferase assays on HEK293 cells plated in 3,9 cm^2 multiwell plate, transfected with increasing doses of pCS2-FLAG-$KRas^{G12V}$ and pcDNA-HER2-V659E, or empty vector (ø). Cells were co-transfected with pGL3b-CTGF-Lux or pGL3b-8xIIG-Lux to test YAP/TAZ transcriptional activity, and with pRL-TK-Renilla, used to normalize luciferase signal. As specificity control, HEK293 cells were previously depleted of YAP and TAZ by transfection with two independent mixes of siRNAs (siYAP/TAZ#1, in grey and siYAP/TAZ#2, in blue). Data are presented as mean ± SD, results are representative of two independent experiments performed in triplicate.

C: Immunoblot analysis of HEK293 cell lysates, prepared from the same samples analyzed in 3A, to assess YAP/TAZ protein level and siRNA knockdown efficiency. GAPDH serves as loading control.

D: Immunoblot analysis of HEK293 cell lysates, prepared from the same samples analyzed in 3B, to assess YAP/TAZ protein levels. GAPDH serves as loading control. Knockdown efficiency was assessed as in C (data not shown).

E: qRT-PCR for *Yap* and *Taz* mRNA expression in HEK293 cells, transfected with pCS2-FLAG-$KRas^{G12V}$ (2,5 ng/cm^2), pcDNA-HER2-V659E (62,5 ng/cm^2), or empty vector (ø, 62,5 ng/cm^2). Data were normalized to *Gapdh* expression levels and presented as mean + SD, results are representative of two independent experiments performed in triplicate.

FIGURE 3

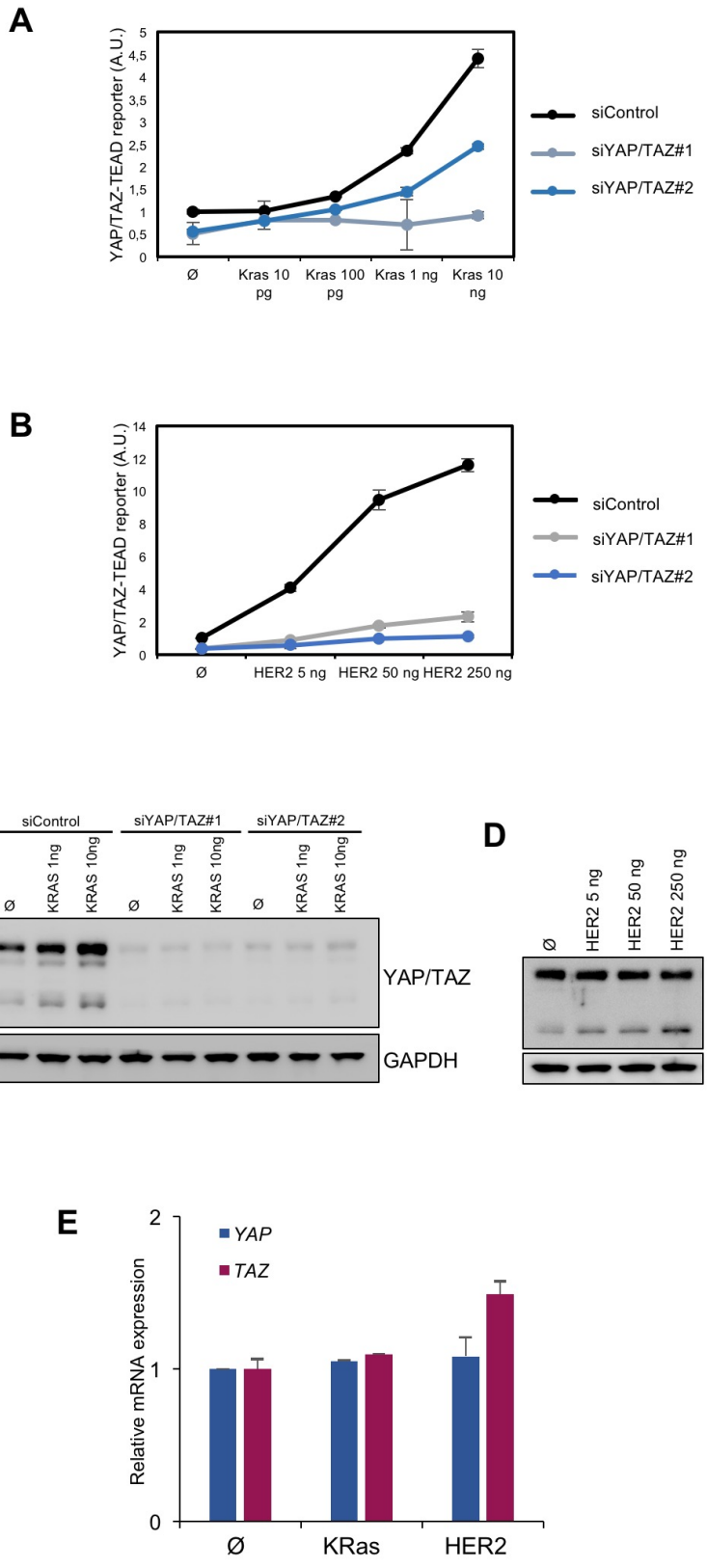
A
YAP/TAZ-TEAD reporter (A.U.)
5
4,5
4
3,5
3
2,5
2
1,5
1
0,5
0
Ø
Kras 10 pg
Kras 100 pg
Kras 1 ng
Kras 10 ng
siControl
siYAP/TAZ#1
siYAP/TAZ#2
B
YAP/TAZ-TEAD reporter (A.U.)
14
12
10
8
6
4
2
0
Ø
HER2 5 ng
HER2 50 ng
HER2 250 ng
siControl
siYAP/TAZ#1
siYAP/TAZ#2
C
siControl
siYAP/TAZ#1
siYAP/TAZ#2
Ø
KRAS 1ng
KRAS 10ng
YAP/TAZ
GAPDH
D
Ø
HER2 5 ng
HER2 50 ng
HER2 250 ng
YAP/TAZ
GAPDH
E
Relative mRNA expression
2
1
0
YAP
TAZ
Ø
KRas
HER2

Figure 4: KRas overexpression promotes YAP/TAZ activity in pancreatic acinar cells

A: Schematic representation of the experiment performed with pancreatic primary cells. Pancreatic acinar cells were isolated from *LSL-KRas^{G12D}* mice, infected with AdenoCre (Ad-Cre) and plated into three-dimensional collagen matrix. Acinar-to-ductal metaplasia (ADM) was scored as the percentage of ductal-like structures appearing in the culture after 5 days.
B: Representative bright field (top panels) and YAP/TAZ immunofluorescence (bottom panels) images of *wt* and *KRas^{G12D}*-mutant cells five days after seeding, as in A. In red, fluorophore-conjugated phalloidin allows to visualize F-actin and assess morphological changes. Nuclei were counterstained with DAPI. Scale bars, 48 μm.
C: qRT-PCR for YAP/TAZ target genes *CYR61* and *CD44* in *wt* and *KRas^{G12D}*-mutant pancreatic cells recovered from collagen five days after seeding. Data were normalized to *18S-rRNA* levels and presented as mean + SD, results are representative of two independent experiments performed in triplicate.

FIGURE 4

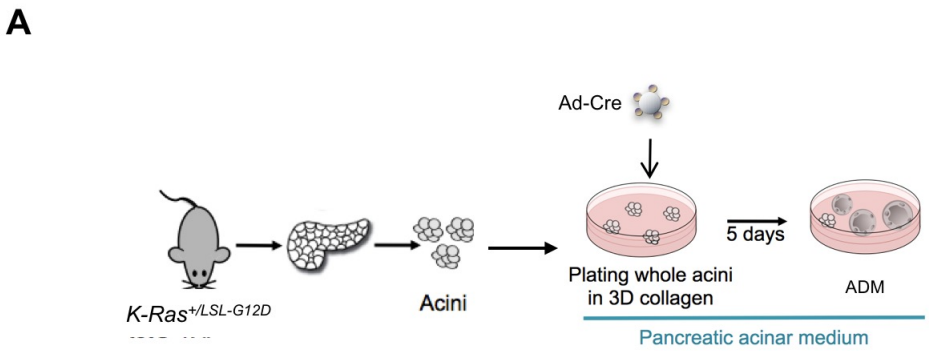
A
Ad-Cre
5 days
Plating whole acini
in 3D collagen
ADM
Acini
K-Ras+/LSL-G12D
Pancreatic acinar medium

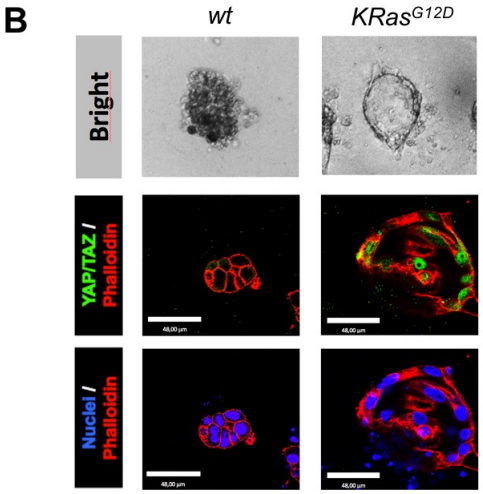
B
wt
KRasG12D
Bright
YAP/TAZ /
Phalloidin
Nuclei /
Phalloidin

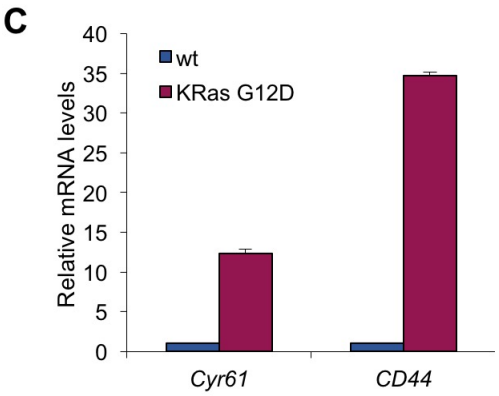
C
Relative mRNA levels
40
35
30
25
20
15
10
5
0
wt
KRas G12D
Cyr61
CD44

Figure 5: YAP/TAZ are required for KRas-mediated Acinar-to-Ductal Metaplasia

A: Schematic representation of the experiment performed with pancreatic primary cells. Pancreatic acinar cells were isolated from *LSL-KRas^{G12}; Yap$^{fl/fl}$; Taz$^{fl/fl}$* mice, infected with AdenoCre (Ad-Cre) and plated into three-dimensional collagen matrix. Acinar-to-ductal metaplasia (ADM) was scored as the percentage of ductal-like structures appearing in the culture after 5 days.

B: Representative bright field and immunofluorescence images of primary pancreatic cells five days after seeding. In red, fluorophore-conjugated phalloidin allows to visualize F-actin. Nuclei were counterstained with DAPI. Scale bars, 50 μm.

C: Quantification of the percentage of ADM events occurring in primary acinar cells expressing mutant KRas alone, or concomitantly depleted of YAP/TAZ (*Yap/Taz* KO). The percentage derives from the number of ductal-like structures normalized to the total number of acinar clusters seeded. Data are presented as mean + SD, results are representative of three independent experiments performed in duplicate.

D: Representative immunofluorescence images of primary pancreatic cells five days after seeding, to assess proliferation rates based on the proliferation marker Ki67. In red, fluorophore-conjugated phalloidin allows to visualize F-actin. Nuclei were counterstained with DAPI. Scale bars, 50 μm.

E: Representative hematoxylin and eosin staining of sections from pancreata of mice of the indicated genotypes (*Ptf1aCre^{ERTM}* or *Ptf1aCre^{ERTM};LSL-KRas^{G12D}* or *Ptf1aCre^{ERTM};LSL-KRas^{G12};Yap$^{fl/fl}$;Taz$^{fl/fl}$)*. Mice were treated with tamoxifen by intraperitoneal injection and pancreata were collected six months after injection. Images show inhibition of tumor formation in KRas-mutant pancreata upon YAP/TAZ depletion.

F: Quantification of the ratio of tumor area, normalized to the total area of the section of pancreata collected from mice treated as in E.

FIGURE 5

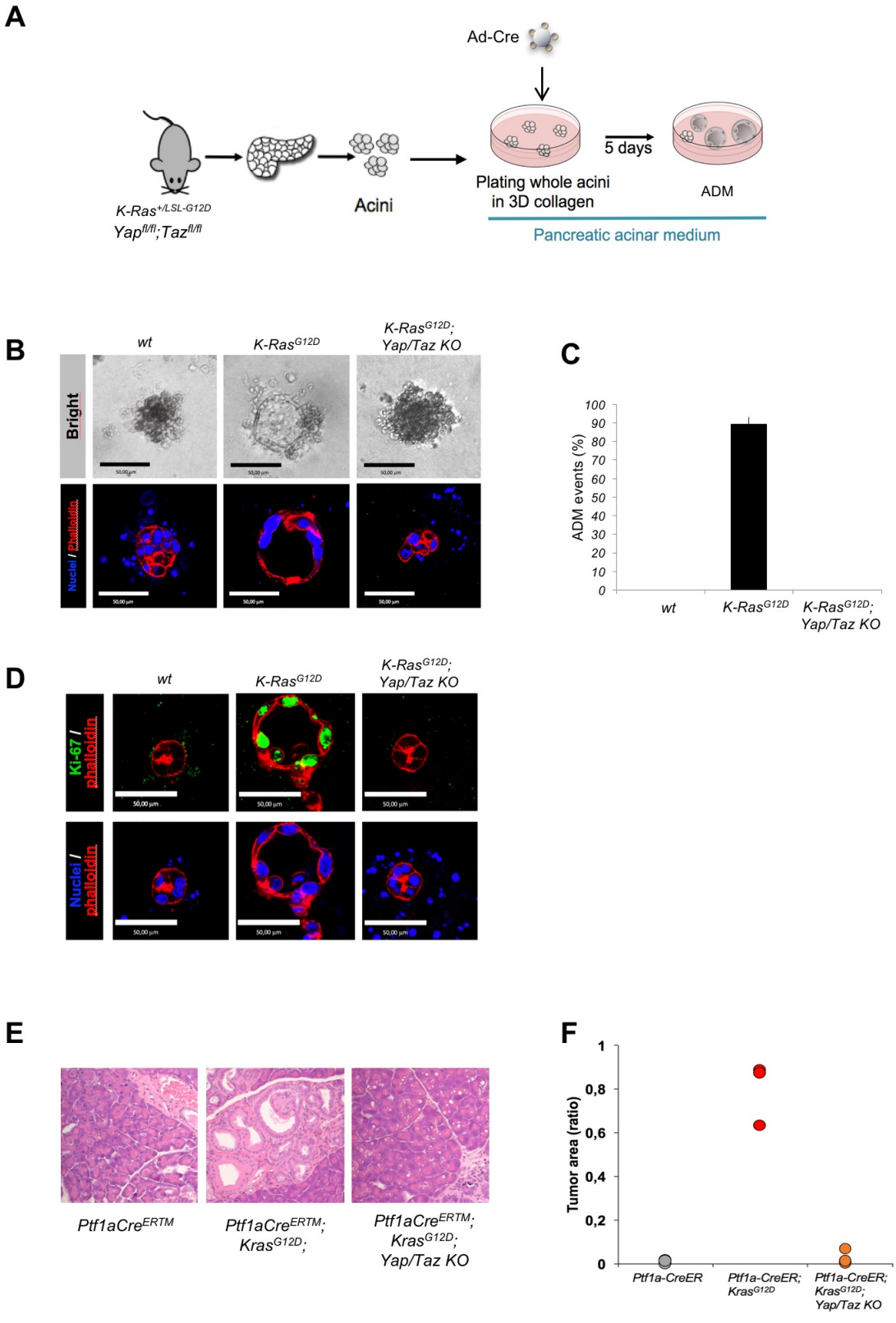
A
Ad-Cre
5 days
K-Ras+/LSL-G12D
Yapfl/fl;Tazfl/fl
Acini
Plating whole acini
in 3D collagen
ADM
Pancreatic acinar medium
B
wt
K-RasG12D
K-RasG12D;
Yap/Taz KO
Bright
Nuclei / Phalloidin
C
ADM events (%)
100
90
80
70
60
50
40
30
20
10
0
wt
K-RasG12D
K-RasG12D;
Yap/Taz KO
D
wt
K-RasG12D
K-RasG12D;
Yap/Taz KO
Ki-67 /
phalloidin
Nuclei /
phalloidin
E
PtfaCreERTM
Ptf1aCreERTM;
KrasG12D;
Ptf1aCreERTM;
KrasG12D;
Yap/Taz KO
F
Tumor area (ratio)
1
0,8
0,6
0,4
0,2
0
Ptf1a-CreER
Ptf1a-CreER;
KrasG12D
Ptf1a-CreER;
KrasG12D;
Yap/Taz KO

Figure 6: HER2 overexpression promotes cell plasticity in adult mammary luminal cells

A: Representative FACS profile illustrating the distribution of Lin–/ EpCAM+ mammary cells according to their CD49f/ CD61 antigenic profile, used to separate three subpopulations: MaSC-enriched fraction ($EpCAM^{low}CD49f^{high}CD61^{+}$), luminal progenitors ($EpCAM^{high}CD49f^{low}CD61^{+}$), and luminal differentiated cells ($EpCAM^{high}CD49f^{low}CD61^{-}$).

B: Schematic representation of the experiments performed with mammary luminal cells: after FACS purification, cells were plated on collagen I-coated plates, transduced with lentiviral vectors encoding for rtTA and for constitutive active HER2, and treated with doxycycline (DOXY) to induce exogenous gene expression. After one week in culture, cells were trypsinized and replated in 5% matrigel-containing clonogenic suspension cultures to assess colony formation.

C: Representative images and quantifications of mammary colonies formed by the indicated cells 15 days after plating in clonogenic medium. The data are presented as mean + SD, results are representative of three independent experiments performed in duplicate. Scale bars, 50 μm.

D: Quantifications of the self-renewal capacity of mammary colonies, measured as the number of colonies that re-grew after dissociation of primary colonies and replating of 2000 cells per well. Data are presented as mean + SD, results are representative of three independent experiments performed in duplicate.

FIGURE 6

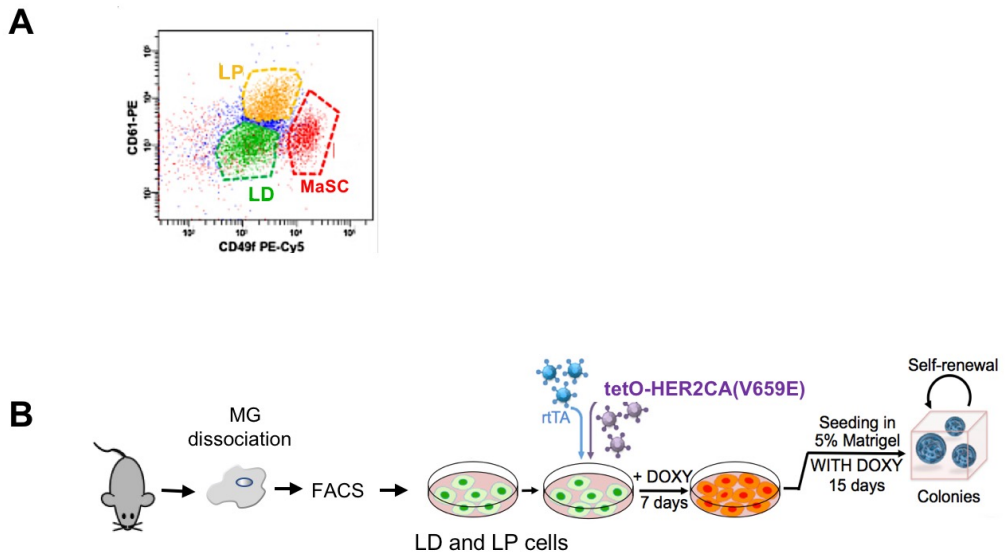
A
LP
LD
MaSC
CD61-PE
CD49f PE-Cy5
B
MG dissociation
FACS
LD and LP cells
rtTA
tetO-HER2CA(V659E)
+ DOXY
7 days
Seeding in 5% Matrigel WITH DOXY 15 days
Self-renewal
Colonies
C
MaSCs
LD cells: rtTA
empty
HER2
LP cells: rtTA
empty
HER2
# of I°ary colonies / 2000 cells
MaSCs
empty
HER2
empty
HER2
LD cells: rtTA
LP cells: rtTA
+doxycycline
D
# of I°ary colonies / 2000 cells
MaSCs
HER2 - DOXY
HER2 + DOXY
HER2 - DOXY
HER2 + DOXY
LD cells: rtTA
LP cells: rtTA
# of II°ary colonies / 2000 cells
MaSCs
HER2 - DOXY
HER2 + DOXY
HER2 - DOXY
HER2 + DOXY
LD cells: rtTA
LP cells: rtTA

Figure 7: YAP/TAZ are required for cell plasticity promoted by HER2 overexpression

A: Schematic representation of the experiments performed with luminal cells collected from mammary gland of mice bearing *Yap*$^{fl/fl}$*; Taz*$^{fl/fl}$ alleles: after FACS purification, cells were seeded on collagen I-coated plates, and transduced with lentiviral vectors encoding for rtTA and for constitutive active HER2 and with an adenoviral vector encoding for the Cre recombinase (Ad-Cre). After one week in culture in the presence of doxycycline (DOXY) to ensure exogenous gene expression, cells were trypsinized and replated in 5% matrigel-containing clonogenic medium to assess colony formation.

B-C: Quantifications of the colony-forming capacity of the indicated mammary cells, 15 days after plating in clonogenic medium. Both LD and LP cells depleted of YAP/TAZ (Ad-Cre +) were unable to form MaSC-like colonies, similarly to control cells transduced with empty vector. Data are presented as mean + SD, results are representative of two independent experiments performed in duplicate.

FIGURE 7

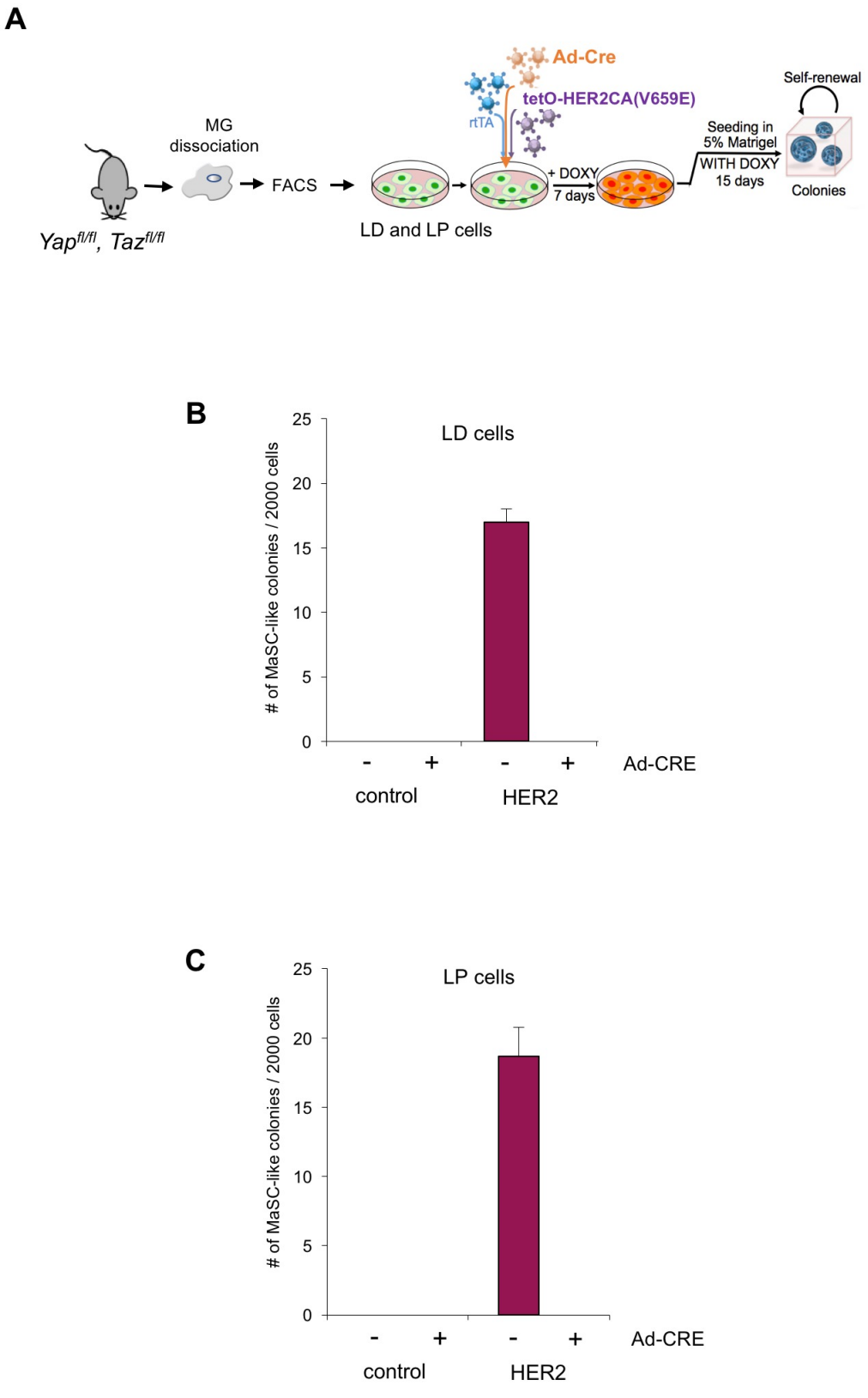
A
Ad-Cre
tetO-HER2CA(V659E)
rtTA
MG
dissociation
FACS
Yap^fl/fl, Taz^fl/fl
LD and LP cells
+ DOXY
7 days
Seeding in
5% Matrigel
WITH DOXY
15 days
Self-renewal
Colonies
B
LD cells
# of MaSC-like colonies / 2000 cells
25
20
15
10
5
0
- + - +
Ad-CRE
control
HER2
C
LP cells
# of MaSC-like colonies / 2000 cells
25
20
15
10
5
0
- + - +
Ad-CRE
control
HER2

Figure 8: KRas tumorigenic effect requires YAP/TAZ mechanotransduction

A-B: Schematic representation of the process of polymerization of PEG-based hydrogels: Polymeric chains based on a four-arm PEG polymer are covalently bound by crosslinker peptides, through a Michael addition reaction. These hydrogels also contain RGD-peptides, to allow cell-matrix adhesion (A). To precisely control the timing of the reaction, and allow to mix and seed cells into the hydrogel before its polymerization, an UV-sensitive photointiator is added, to catalyze the Michael addition only upon UV light exposure (B). Modified from Brusatin et al., 2018.

C: Bright field images of KRas mutant pancreatic primary cells embedded in PEG-based hydrogels of the indicated stiffness.

D: Quantification of the percentage of ADM events occurring in primary acinar cells expressing mutant KRas, seeded in the same condition of C. The percentage derives from the number of ductal-like structures normalized to the total number of acinar clusters seeded. Data are presented as mean + SD, results are representative of two independent experiments performed in duplicate.

E-F: Bright field images and quantification (in F, measured as in D) of KRas mutant pancreatic primary cells embedded in collagen-based matrix and treated with two different doses of Latrunculin A (LatA) and CytochalasinD (CytoD). High dose: 2μM Low dose: 200 nM.

FIGURE 8

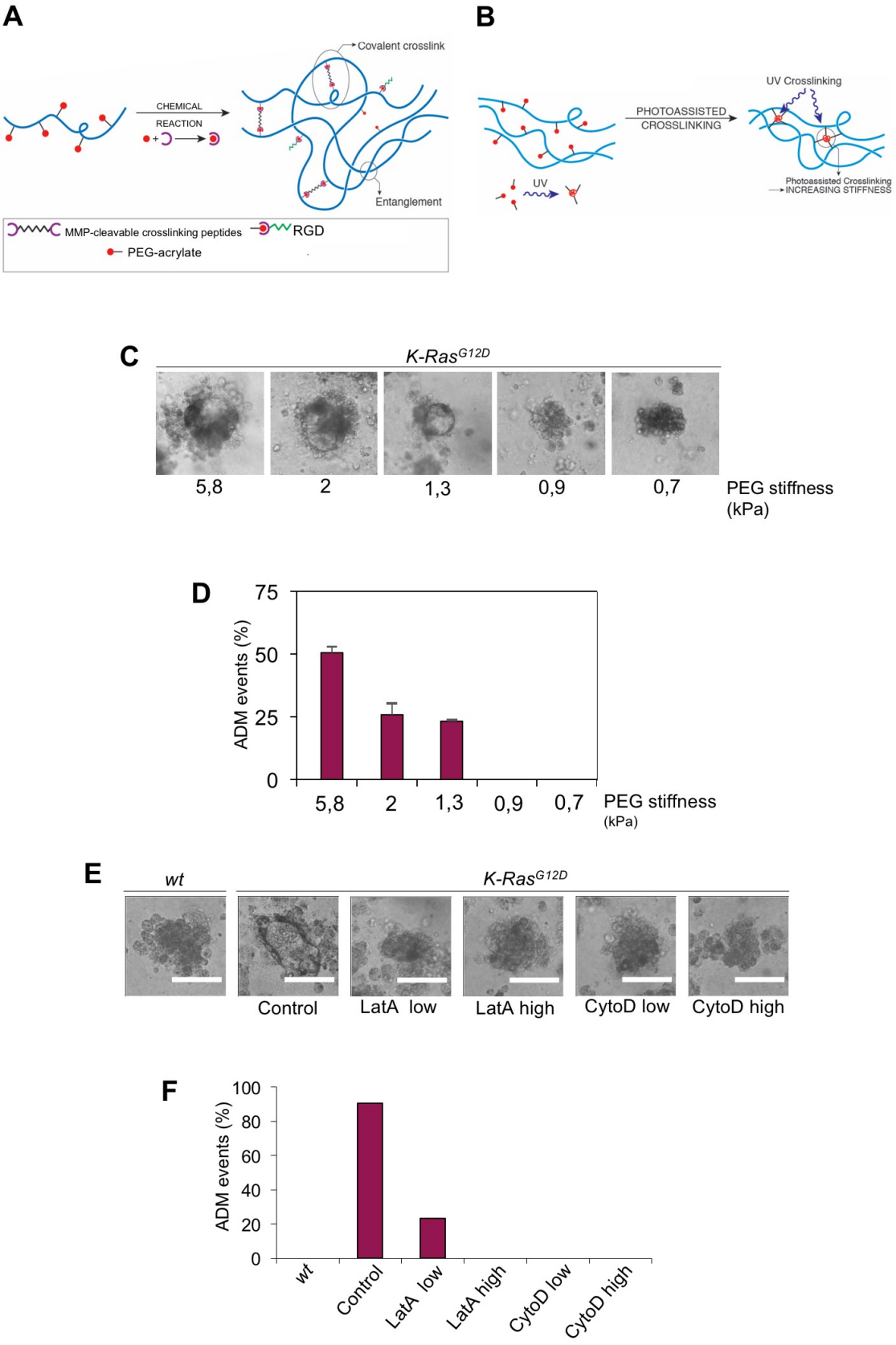
A
Covalent crosslink
CHEMICAL
REACTION
Entanglement
MMP-cleavable crosslinking peptides
RGD
PEG-acrylate
B
UV Crosslinking
PHOTOASSISTED
CROSSLINKING
UV
Photoassisted Crosslinking
INCREASING STIFFNESS
C
K-RasG12D
5,8
2
1,3
0,9
0,7
PEG stiffness
(kPa)
D
ADM events (%)
75
50
25
0
5,8
2
1,3
0,9
0,7
PEG stiffness
(kPa)
E
wt
K-RasG12D
Control
LatA low
LatA high
CytoD low
CytoD high
F
ADM events (%)
100
80
60
40
20
0
wt
Control
LatA low
LatA high
CytoD low
CytoD high

Figure 9: Defactinib and Dasatinib efficiently inhibit KRas-induced ADM by blunting YAP/TAZ activity.

A: Representative bright field images of primary pancreatic acinar cells collected from mice of the indicated genotypes *(LSL-KRas^{G12D}* or *LSL-KRas^{G12};R26-rtTAM2;TetO-YAP^{S127A})* and treated with Defactinib (10 μM) or Dasatinib (100nM), concomitantly with doxycycline to activate YAP expression, for five days. Scale bars, 400 μm.

B: Quantification of the percentage of ADM events occurring in primary acinar cells overexpressing mutant KRas alone or in combination with YAP. The percentage derives from the number of ductal-like structures normalized to the total number of acinar clusters seeded. Data are presented as mean + SD, results are representative of two independent experiments performed in duplicate.

C: Immunofluorescence images of primary pancreatic acinar cells five days after seeding, to assess cytoskeletal changes, through phalloidin-staining of F-actin (red), and YAP subcellular localization (green). Nuclei were counterstained with DAPI. Scale bars, 80 μm.

FIGURE 9

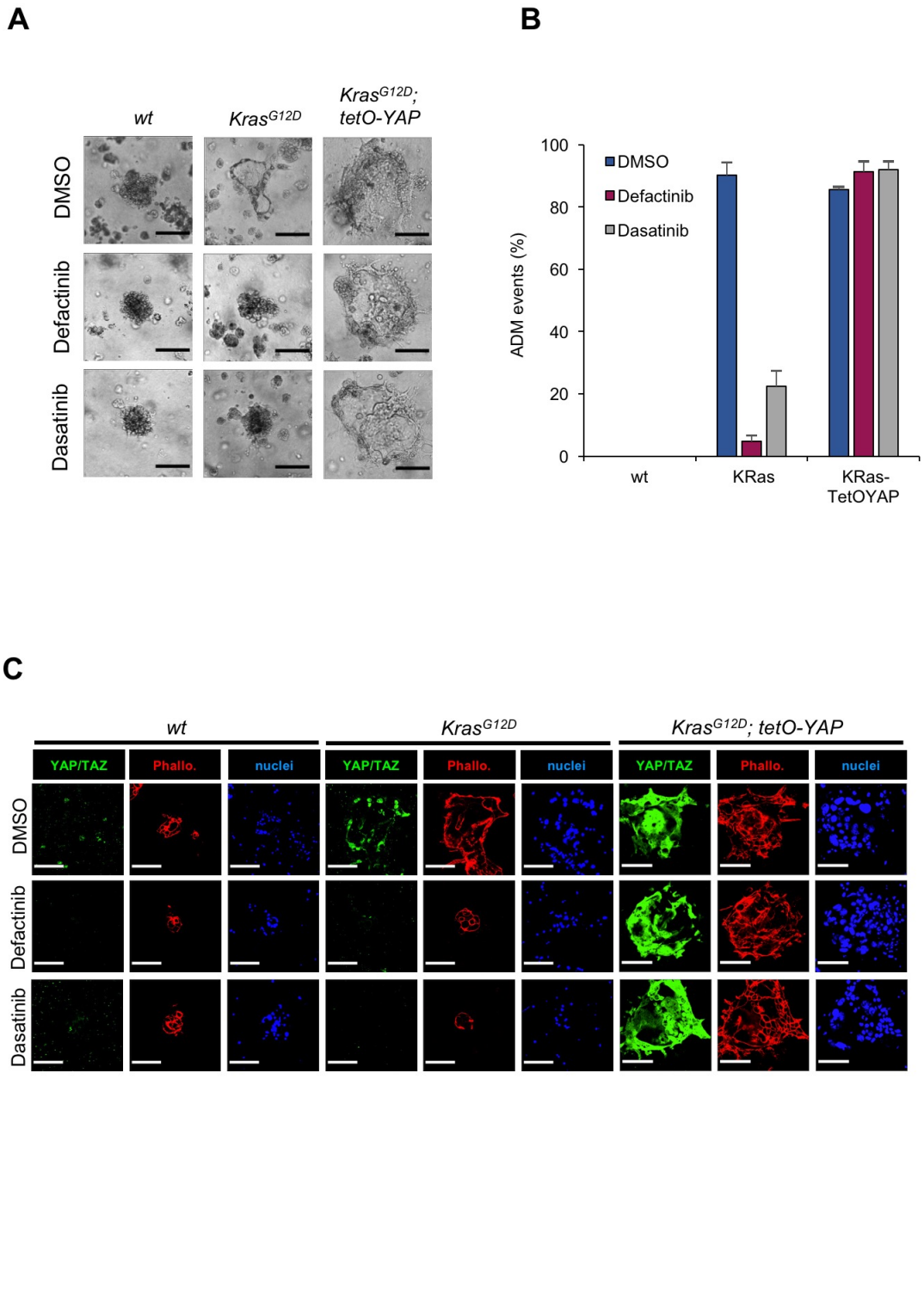
A
wt
KrasG12D
KrasG12D; tetO-YAP
DMSO
Defactinib
Dasatinib
B
ADM events (%)
100
80
60
40
20
0
DMSO
Defactinib
Dasatinib
wt
KRas
KRas-TetOYAP
C
wt
KrasG12D
KrasG12D; tetO-YAP
YAP/TAZ
Phallo.
nuclei
DMSO
Defactinib
Dasatinib

Figure 10: BAPN treatment inhibits mammary carcinoma *in vivo*

A: Schematic representation of the experimental set up carried out to evaluate the effect of the LOX inhibitor BAPN on MMTV-PyMT induced carcinomas. From weaning, female mice were treated with BAPN in drinking water (3mg/ml), for 8 weeks. At experimental endpoint, mammary glands were collected.
B: Representative images of the indicated histological and immunohistochemical stainings of mammary glands dissected from mice of the indicated genotypes, either treated with BAPN or with control water (as described in A). From the top: Hematoxylin-Eosin staining of mammary gland sections, Picrosirius Red staining to visualize collagen fibers, and immunohistochemical staining of Ki67 and YAP.

FIGURE 10

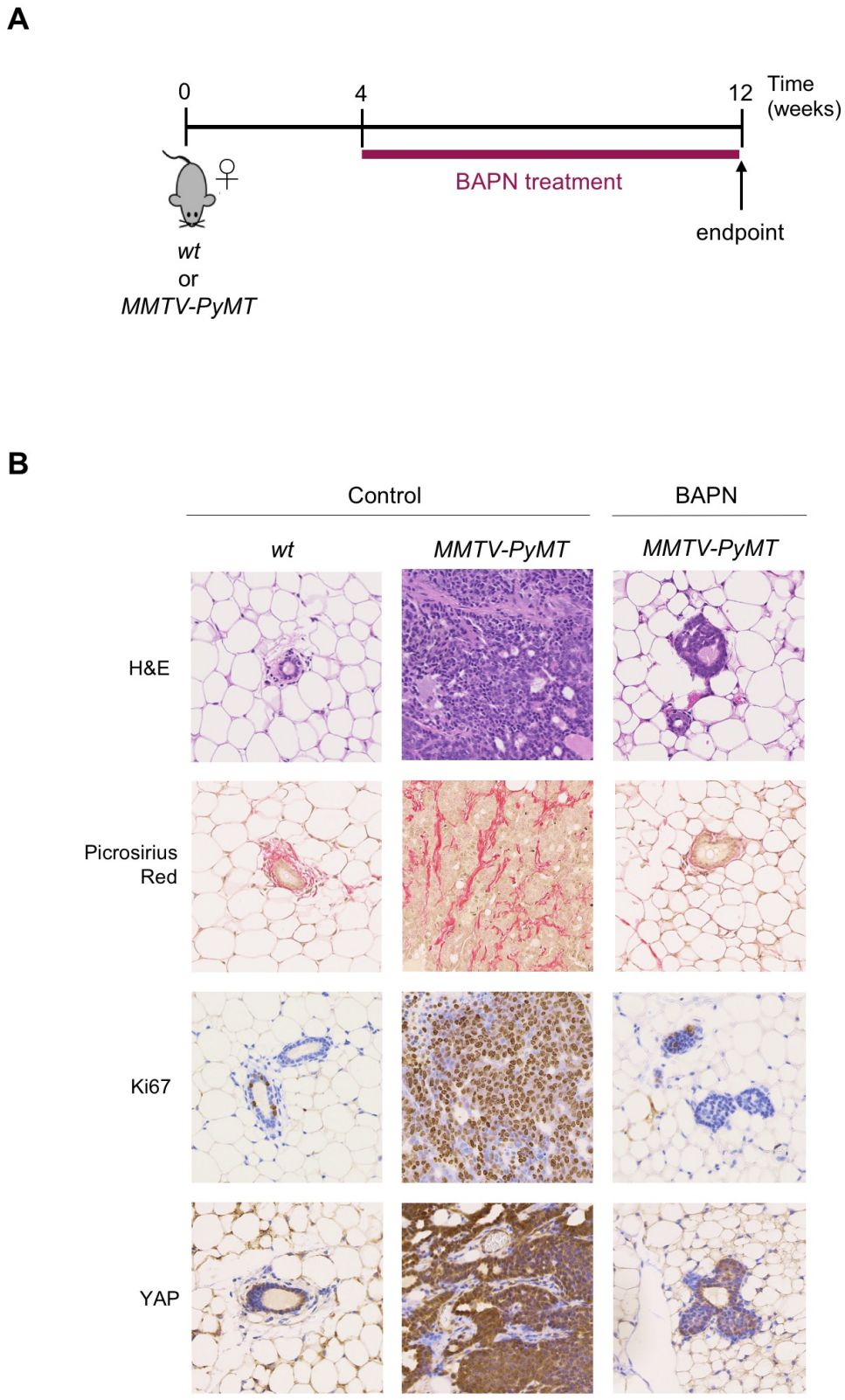
A
0
4
12
Time (weeks)
BAPN treatment
endpoint
wt
or
MMTV-PyMT
B
Control
BAPN
wt
MMTV-PyMT
MMTV-PyMT
H&E
Picrosirius Red
Ki67
YAP

Figure 11: BAPN treatment inhibits pancreatic adenocarcinoma *in vivo*

A: Schematic representation of the experimental set up carried out to evaluate the effect of the LOX inhibitor BAPN on mutant KRas induced carcinomas. At weaning, mice were treated with tamoxifen by intraperitoneal injection (30mg/kg of body weight), and after a week treated with BAPN in drinking water (3mg/ml), for 11 weeks. At experimental endpoint, pancreata were collected.

B: Representative images of the indicated histological and immunohistochemical stainings of pancreata dissected from mice of the indicated genotypes, either treated with BAPN or with control water (as described in A). From the top: Hematoxylin-Eosin staining of pancreas sections, Picrosirius Red staining to visualize collagen fibers, and immunohistochemical staining of YAP and TAZ.

FIGURE 11

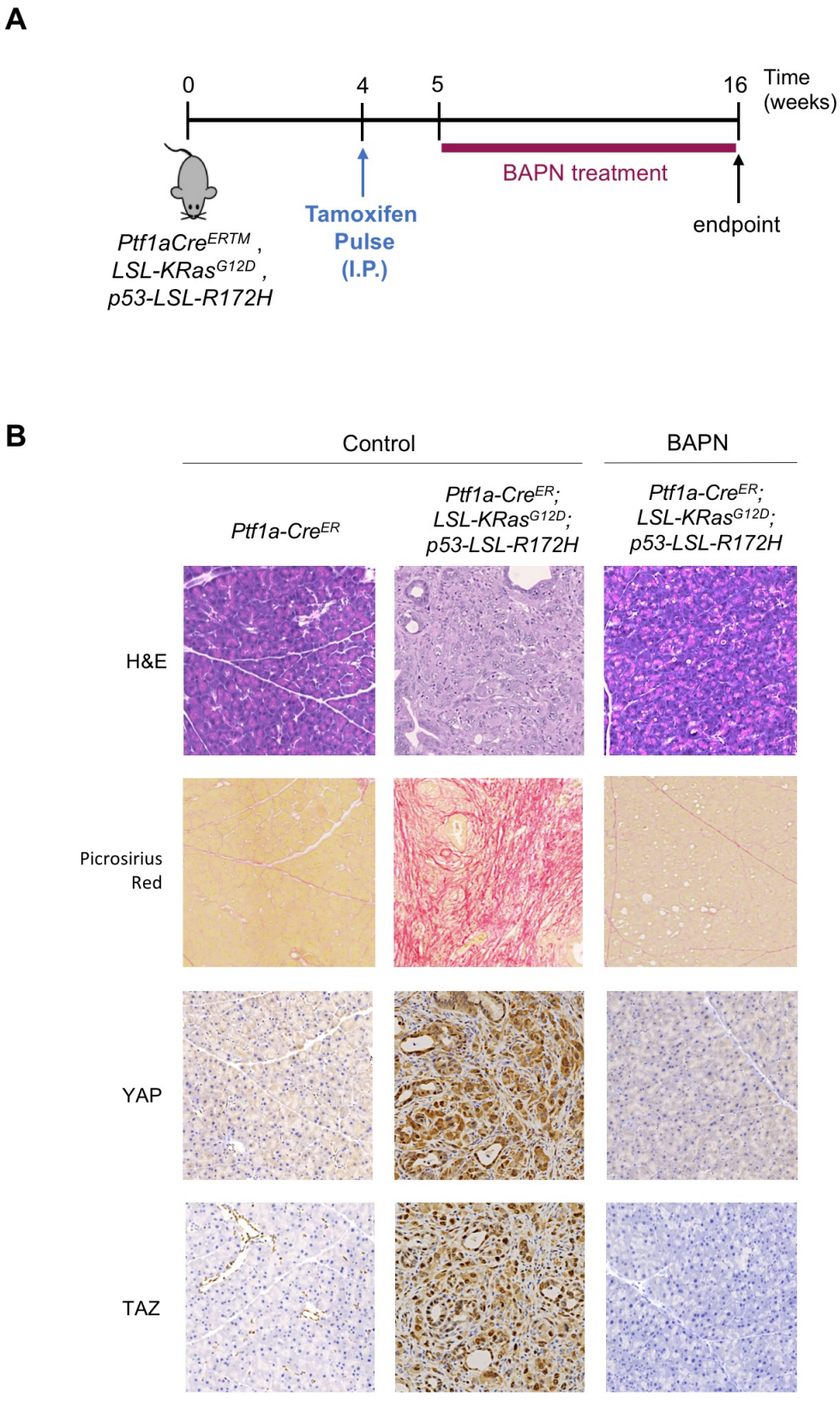
A
0
4
5
16
Time (weeks)
BAPN treatment
endpoint
Tamoxifen Pulse (I.P.)
Ptf1aCreERTM , LSL-KRasG12D , p53-LSL-R172H
B
Control
BAPN
Ptf1a-CreER
Ptf1a-CreER; LSL-KRasG12D; p53-LSL-R172H
Ptf1a-CreER; LSL-KRasG12D; p53-LSL-R172H
H&E
Picrosirius Red
YAP
TAZ

Figure 12: Angiomotin proteins are YAP/TAZ inhibitors in classical mechano-assays

A: Luciferase assay on HEK293T cells, transfected with YAP/TAZ-TEAD luciferase reporter and with a plasmid encoding for Renilla to normalize luciferase signal. To test the effect of Angiomotins loss, cells were previously depleted of all the members of the motin family by transfections with two independent mixes of siRNAs. Cells were then plated on polyacrylamide gels (0,7 kPa, SOFT) or on fibronectin-coated plastic (STIFF), as positive control for YAP/TAZ activation. Data are presented as mean + SD, results are representative of three independent experiments performed in duplicate.
B: Luciferase assay on HEK293T cells, transfected with YAP/TAZ-TEAD luciferase reporter and with a plasmid encoding for Renilla to normalize luciferase signal. To test the effect of AMOT overexpression, cells were co-transfected with a plasmid encoding for AMOTwt. Cells were then plated at high confluence (DENSE) or at low confluence (SPARSE) as positive control for YAP/TAZ activation. Data are presented as mean + SD, results are representative of three independent experiments performed in triplicate.
C: Representative immunofluorescence images of HEK293T cells plated at the indicated confluences, previously depleted of all the members of the motin family by transfections with two independent mixes of siRNAs.
D: Quantification of the percentage of cells treated as in C, that show nuclear (N), evenly distributed (N/C) or cytoplasmic (C) YAP/TAZ subcellular localization.

FIGURE 12

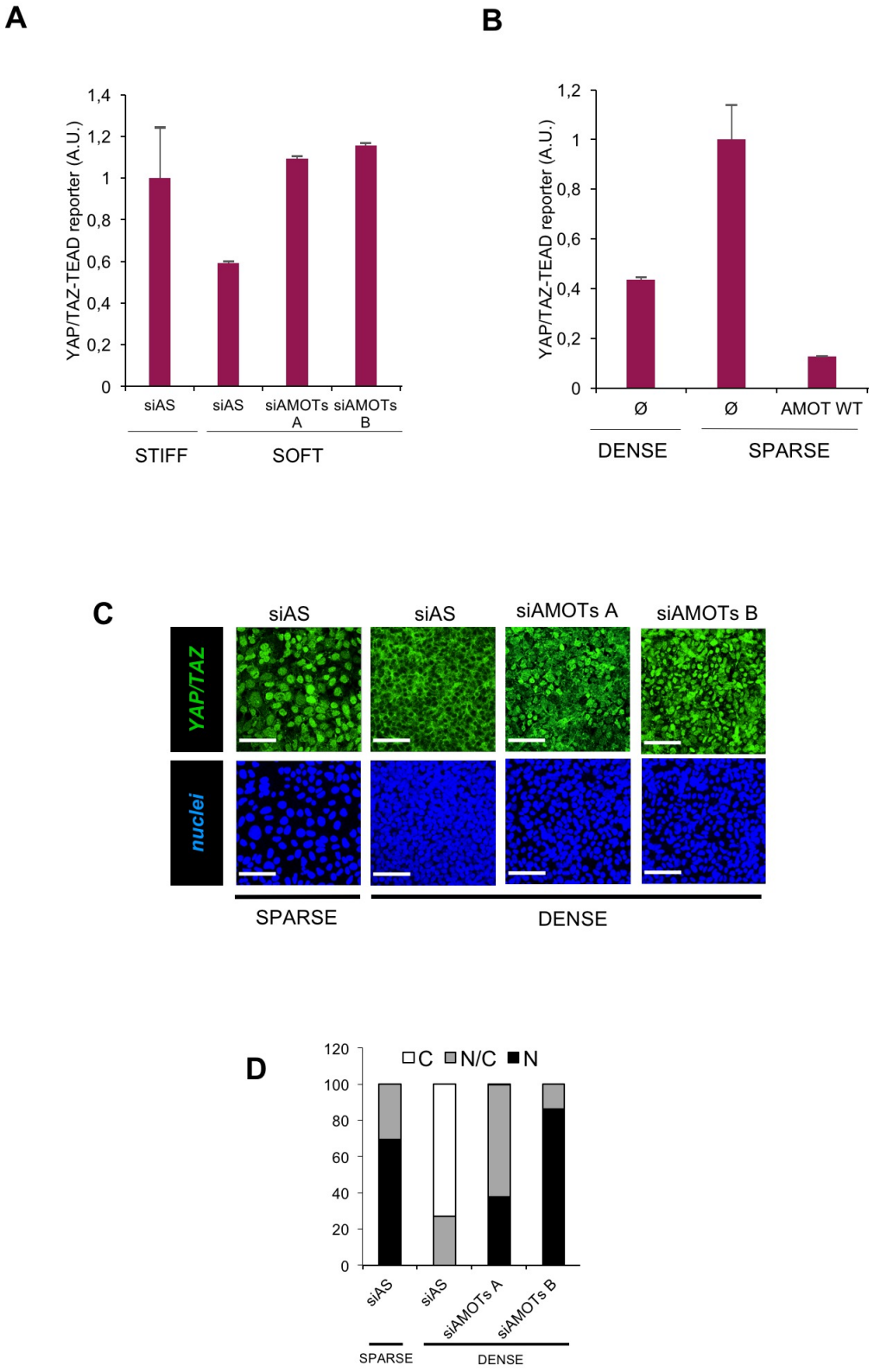
A
YAP/TAZ-TEAD reporter (A.U.)
1,4
1,2
1
0,8
0,6
0,4
0,2
0
siAS
siAS
siAMOTs A
siAMOTs B
STIFF
SOFT
B
YAP/TAZ-TEAD reporter (A.U.)
1,2
1
0,8
0,6
0,4
0,2
0
Ø
Ø
AMOT WT
DENSE
SPARSE
C
siAS
siAS
siAMOTs A
siAMOTs B
YAP/TAZ
nuclei
SPARSE
DENSE
D
C
N/C
N
120
100
80
60
40
20
0
siAS
siAS
siAMOTs A
siAMOTs B
SPARSE
DENSE

Figure 13: AMOT binding to YAP is regulated by cytoskeletal rearrangements

A: Schematic representation of the proposed model for the mechanism of YAP/TAZ inhibition by Angiomotins. In cells that are experiencing high mechanical inputs, and that have a highly polymerized and contractile cytoskeleton (Left panel), AMOT is mostly bound to F-actin fibers; in this condition YAP/TAZ are free to enter the nucleus. On the contrary, in cells that are experiencing low mechanical stress, in which F-actin is less polymerized (right panel), an increased fraction of Angiomotins might be released from the interaction with F-actin, and thus be free to bind YAP/TAZ, inhibiting their nuclear entry.
B: Immunoblot analysis of insoluble and soluble differential extracts of HEK293T cells, treated with phalloidin to stabilize filamentous actin. Upon F-actin stabilization, AMOT protein is re-localized in the insoluble (Ins, F-actin bound) fraction, while in control cells (UNT) it is partially bound to F-actin and partially free in the cytoplasm (Sol, F-actin unbound).
C: Immunoblot analysis of a co-immunoprecipitation assay (IP) assessing the binding of endogenous AMOT to YAP. YAP efficiently immuno-precipitates AMOT, but this interaction is weakened upon F-actin stabilization by Phalloidin treatment (compare lane 1 to lane 2). Compare lane 3 and 4 to lane 1 for controls of IP specificity. Bottom: Inputs showing corresponding total protein levels.

FIGURE 13

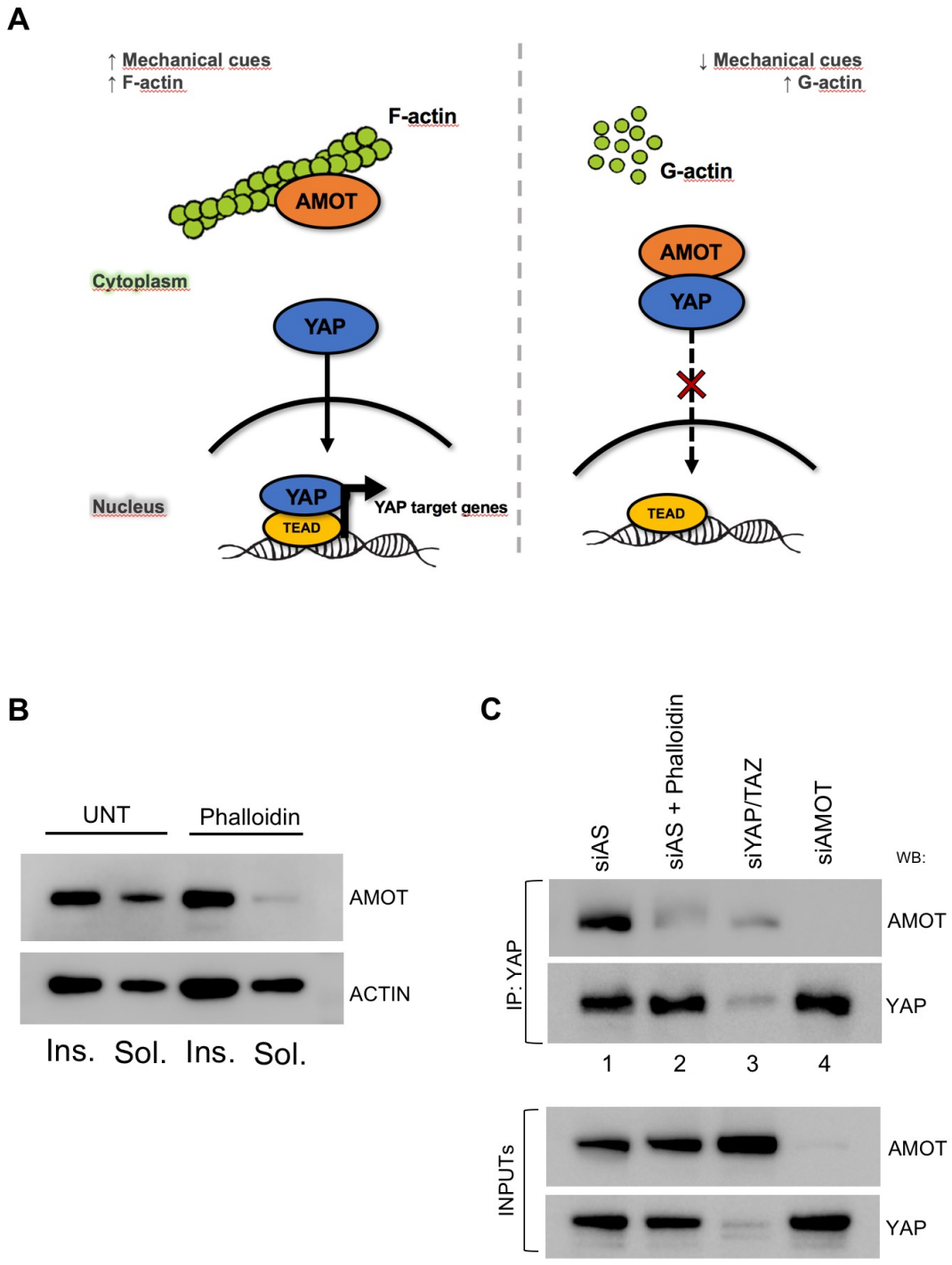
A
↑ Mechanical cues
↑ F-actin
F-actin
AMOT
Cytoplasm
YAP
YAP
TEAD
YAP target genes
Nucleus
↓ Mechanical cues
↑ G-actin
G-actin
AMOT
YAP
TEAD
B
UNT
Phalloidin
AMOT
ACTIN
Ins. Sol. Ins. Sol.
C
siAS
siAS + Phalloidin
siYAP/TAZ
siAMOT
WB:
IP: YAP
AMOT
YAP
1 2 3 4
INPUTs
AMOT
YAP

Acknowledgments

I would like to acknowledge my advisor Prof. Stefano Piccolo, that has always been an inspiring and provocative mentor, and all the members of our lab for the helpful collaboration. In particular special thanks should be given to Dr. Tito Panciera, who developed and carried out the project, and was an essential guide for the realization of this thesis.